REVIEW

Check for updates

Continuous biosignal acquisition beyond the limit of epidermal turnover†

Aman Bhatia, [ID] [a] Kevin Albert Kasper [ID] [a] and Philipp Gutruf [ID] *[abcd]

Acquisition of biosignals is particularly valuable if uninterrupted data streams are collected over weeks or months without gaps. This is currently only possible with devices that feature long battery life and interfaces such as belts and straps that result in substantial limitations for signal fidelity, sensor location, wear comfort and user retention. State of the art patch-type wearables provide advanced sensing modalities, however, they require adhesives that need to frequently be replaced because of epidermal turnover and pose related limits for chronic operation. This review explores the value of chronic data streams to diagnostics and therapeutics with a detailed dissection of current sensors for chronic applications, system level architectures, sensing modalities and electronic concepts that enable continuous 24/7 high-fidelity insight into physiology.

Wider impact

Existing reviews primarily focus on wearable sensors, their materials, skin interfaces, and applications. However, few address the unique challenges and solutions associated with chronic use, defined as continuous operation over weeks. This review fills that gap by providing a comprehensive overview of strategies for long-term operation. It explores the necessary advances in materials science, sensor technology, and biomedical integration required to maintain uninterrupted biosignal acquisition with clinical-grade fidelity. Additionally, it examines the impact of sustained data availability on clinical applications and patient outcomes.

[a] Department of Biomedical Engineering, The University of Arizona, Tucson, AZ 85721, USA. E-mail: pgutruf@arizona.edu

[b] Department of Electrical and Computer Engineering, The University of Arizona, Tucson, AZ 85721, USA

[c] Bio5 Institute, The University of Arizona, Tucson, AZ 85721, USA

[d] Neuroscience Graduate Interdisciplinary Program (GIDP), The University of Arizona, Tucson, AZ 85721, USA

† Electronic supplementary information (ESI) available. See DOI: https://doi.org/10.1039/d5mh00758e

Aman Bhatia is currently a Post-doctoral Research Associate in the Department of Biomedical Engineering at the University of Arizona, Tucson, AZ, USA. His work focusses on the creation of biosymbiotic electronics, a device class that uses body contours and soft 3D printed elastomers embedded with wirelessly powered electronics to enable intimate contact with the body to realize measurement of biosignals on chronic timescales. He received his PhD in Chemistry

Aman Bhatia

from Pusan National University, Busan, South Korea in 2022. His PhD research focuses on developing electrochemical immunosensors employing catalytic metal deposition and polyenzyme labels. His previous postdoctoral research at Pusan National University focused on developing ferrocene mediated electrochemical glucose sensors.

Kevin Albert Kasper is currently a doctoral candidate in the Department of Biomedical Engineering at the University of Arizona, Tucson, AZ, USA working with Professor Philipp Gutruf on wireless, battery-free, fully implantable electronics. He received his BS in Electrical Engineering from Boston University, Boston, MA, USA in 2017. His PhD research focuses on the integration of ultralow-power, fully implantable battery-free medical devices and wireless, wearable devices for chronic biosensing applications.

Kevin Albert Kasper

1. Introduction

Wearable technologies represent a significant sector of private and federal investment with substantial growth projections at a rate of 30% year over year.[1] Research in this area focuses on exploration of new real-time physiological biosignal acquisition captured through noninvasive monitoring of biophysical,[2] biochemical,[3] and electrophysiological[2,4] markers captured with optical,[2] mechanical[5] and electrical signatures in media such as sweat, tissues and interstitial fluid.[6] Recent efforts have advanced the way biosignals are monitored, offering potentially unprecedented advances in diagnostics, therapeutics, and human–machine interfaces.[7–10] While current sensing modalities offer exciting new insights over short operational times demonstrated in controlled environments, they often face significant barriers in power supply, data management, and biointerface design which collectively limit their operational time and user comfort, limiting translational potential and negatively impacting user retention.[11,12] Addressing these challenges is essential to unlocking the full potential of wearable devices, enabling the digital health paradigm and advancing diagnostics and therapeutics.[13]

Consequently, this review examines the current state of the art of wearable technologies and their aptitude towards continuous sensing ability and opportunities for expansion thereof. Specifically, innovations in biointerfaces, power strategies, biosensing modalities, and data analysis that address the limitations of operation time on the subject are reviewed. Furthermore, the clinical utility of such systems is discussed, highlighting their role in diagnostics, personalized therapy, and seamless integration into healthcare workflows.

Philipp Gutruf

Philipp Gutruf is an Associate Professor in the Biomedical Engineering Department, Craig M. Berge Faculty Fellow at the University of Arizona. In the last 5 years his lab has authored over 50 peer reviewed journal articles, 14 patents and his work has been highlighted on 8 journal covers. He has also been the recipient of prestigious scholarships and fellowships such as the 2024 daVinci Fellowship, International Postgraduate Research Scholarship (IPRS) and the Australian Nano Technology Network Travel Fellowship. His research group focuses on creating devices that intimately integrate with biological systems by combining innovations in soft materials, photonics and electronics to create systems with broad impact on health diagnostics, therapeutics and exploratory neuroscience.

2. Fundamental limitations to operation time of wearable devices

Wearable devices capable of continuously collecting high-fidelity biosignals over weeks or months are becoming increasingly valuable because of modern data analysis methodologies.[14] However, their operation time is constrained by several interconnected factors that impact performance, longevity, and user experience.[15] Power supply limitations dictate how long a device can function before requiring recharging or replacement, while the handling of continuous data streams and storage presents challenges in managing large volumes of information without compromising efficacy. Efficient data analysis is essential for extracting meaningful insights in real time, but computational demands can accelerate power consumption and perpetuate processing delays. Biointerface considerations, including the device's body location and integration strategy, directly affect signal quality and user comfort over extended use. Additionally, the durability of materials and biosensors is critical for maintaining accurate measurements under physical stress and environmental exposure. The development of next-generation wearable electronics for chronic applications hinges heavily on addressing the challenges holistically as devices approach new limitations. Fig. 1 shows an overview of these fundamental limitations to operation time, with a review of capabilities over a span of 2 weeks and a breakdown of continuous 24-hour operation.

2.1. Data storage and streams

Efficient data stream management and storage are essential for continuous operation of wearable devices, particularly in remote and low-resource environments. The most prevalent implementations of low power communication are medium- to long-range, *e.g.*, BLE, LoRa, Zigbee, WiFi and emerging passive BLE,[16–18] do not require proximal contact with the device, thereby allowing for continuous communication during daily routines. Most prevalent embodiments feature distinct trade-offs over a 14-day period: bluetooth low energy (BLE) and long-range (LoRa) communication exhibit data fidelity, and transmission range as shown in Fig. 1: data storage and streams. BLE, while offering high data transfer rates (1.3 Mbps in practice),[19] has noticeable peak power demands (typically ∼10–30 mW depending on chipset)[19,20] and relies on proximity to personal devices for data transmission. Its intermittent connectivity limits its use for long-term, uninterrupted monitoring and often requires pairing with temporary data storage on device.[21–23] In contrast, LoRa facilitates continuous data streaming by leveraging low-power, wide-area network (LPWAN) capabilities. It supports data rates in the range of 0.3–100 kbps, depending on spreading factor and bandwidth.[24] This extended operation distance comes at the cost of reduced data rate, which constrains the complexity and volume of transmitted information. These trade-offs reflect broader challenges in wearable technology development, where conventional communication protocols, such as BLE and Wi-Fi, are robust but often impractical in areas lacking reliable infrastructure.[14,25]
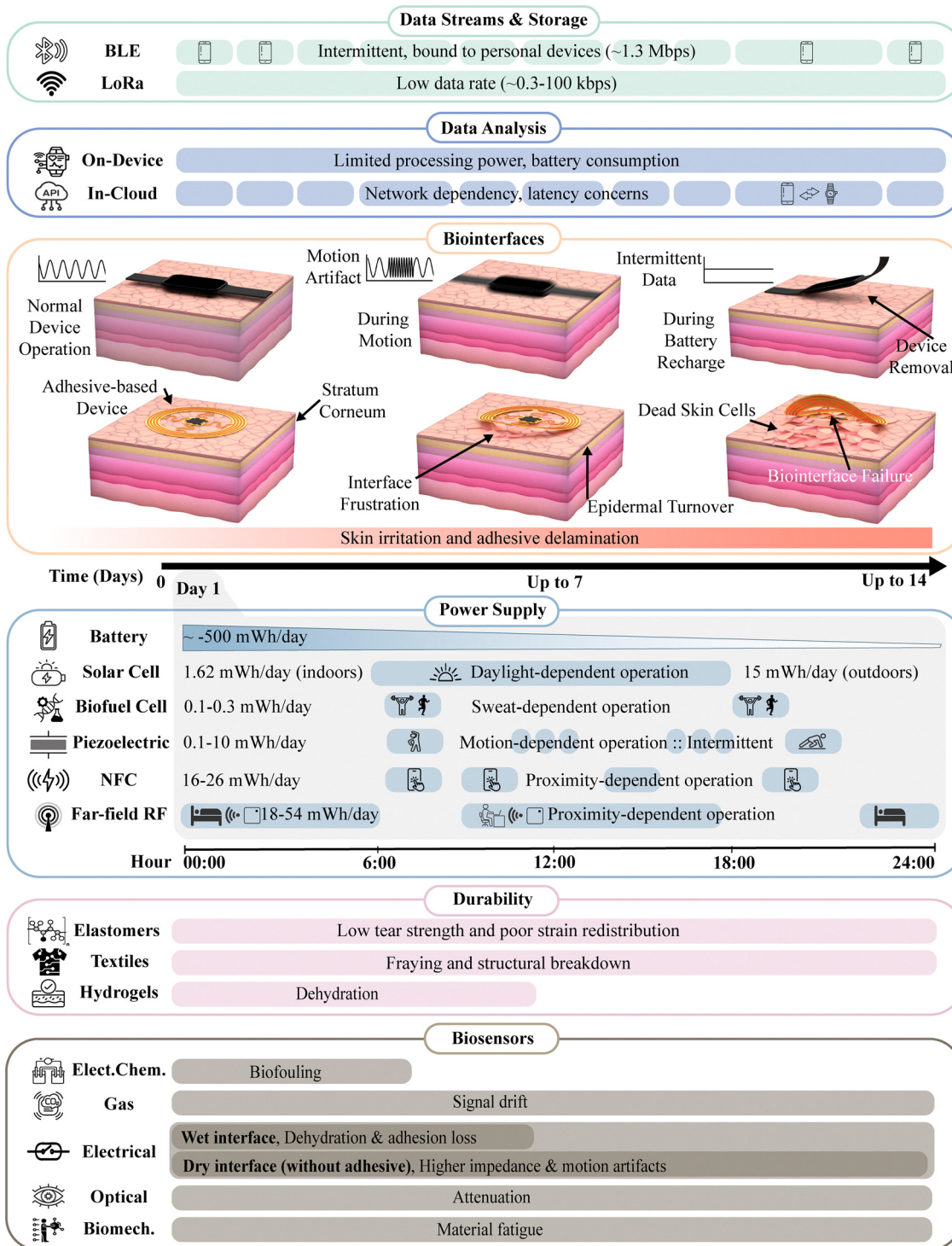
Fig. 1 Fundamental limitations to operation time of wearable devices: illustration showing key factors limiting the operational lifespan of wearable devices, including energy constraints, data flow and storage capacity, processing efficiency, body attachment and integration methods, material longevity, and sensor performance. Image for "Biointerfaces": reproduced from ref. 14 with permission from AIP Publishing, Copyright 2022.

LPWAN protocols like LoRa offer a promising solution for long-range, low-power data transmission, enabling wearable devices to function effectively in remote and supervised care settings in distributed living arrangements without infrastructure in every habitat.[26,27] However, integrating these technologies into wearable platforms remains challenging due to the high peak power requirements ($\sim$46–490 mW Tx, $\sim$20–129 mW Rx)[23,28] resulting in the need for batteries capable of delivering high current and larger antennas, which increase device size.[29,30]

As devices move toward chronic operation times with less user interaction, communication abilities need to improve. BLE works well when consistent infrastructure such as smart phones are present and day-long operation with routine charging times and data offloading is an option, however in settings where connectivity is not always a given, such as in assisted care, in-patient facilities and aged care, new capabilities in communication like LoRa embedded in wearables, enable advanced capabilities to bridge the digital divide.[31–33]

2.2. Data analysis

The choice between on-device and cloud-based data analysis in wearable systems as shown in Fig. 1: data analysis section presents a complex trade-off between data transmission efficiency, communication distance, and analytical complexity.[34] On-device analysis enables real-time data processing with minimal data transmission, making it suitable for continuous monitoring in scenarios where low data rates are sufficient. This promotes communication protocols such as chirped spread spectrum, the enabling technology behind long range protocols such as LoRa, that trade off time of transmission event to achieve long communication distances. This reduces the reliance on external networks, ensuring reliable operation even in areas with limited connectivity. However, on-device processing is constrained by the computational capacity of the device, which is proportional with energy availability, limiting the complexity of the analysis.[35,36]

In contrast, cloud-based analysis leverages high computational power, allowing for more sophisticated data analysis and multimodal data source integration. This approach is particularly advantageous for handling large datasets or applying complex machine learning algorithms. However, it requires higher data rate transmission from the wearables and reliable communication or extensive onboard storage, which introduces dependencies on network availability and increases the risk of latency and data synchronization issues, providing a challenge for applications where many devices need to be networked. Consequently, the trade-off between on-device and cloud-based analysis depends on the specific application needs, whether prioritizing capabilities of initial data analysis, power availability on device, connection infrastructure, and user burden.[37,38]

2.3. Biointerface

Battery-powered wearables, like smartwatches and fitness trackers, face limitations in sensing quality, usability, and user compliance[39,40] as shown in Fig. 1: biointerface section. The device bulk results in motion artifacts and slow response rate due to thermal and mechanical mass,[41–43] and frequent need for recharging, specifically adhesive-based systems often complicate battery recharge logistics, requiring device removal or proximity wireless charging that interrupts continuous use (Table S1, ESI†), that disrupts biosignal collection, leading to data loss[44] and reduction in device relevance for the user, ultimately leading to discontinued use.[45] Ease of device use plays a key role in user acceptance of wearables, where high

fidelity monitoring with clinically relevant biosignal quality is required, alongside minimal burden of use, e.g., charging, cleaning, and adhesive replacement, for impact on diagnostics and therapeutics.[46,47]

In comparison to brick and strap devices, epidermal electronics offer skin-like flexibility and low profiles, enabling substantially better biosignal acquisition and because of the freedom of placement allowing physiological locations that enable higher signal quality. Additionally, because of the low profiles they allow for large device size,[48–51] which increases material choice and contact area, substantially expanding application scope. Examples are electrophysiological devices that can provide clinical grade operation with fidelity and capabilities far beyond current traditional approaches.[52–54] However, their reliance on adhesives for skin contact are fundamentally limited by epidermal turnover, resulting in device lifetimes of maximum 7–14 days and requiring frequent replacements that can impact user compliance, especially in at-home settings.[55] Adhesive-based systems, while enabling lower motion artifacts due to conformal contact,[56–58] face challenges as adhesive strength degrades.[59] Skin cell buildup leads to irritation, interface degradation such as increased impedance for electrical contacts, and adhesive failure from sweat results in a limited lifetime highly dependent on the user.[60,61] Strap-based wearables, on the other hand, show high motion artefact due to relative motion of device body, strap and the underlying physiological target, requiring either frequent adjustment or very high contact pressures (Table S1, ESI†).[62–65] Recent advances in epidermal sensor technologies demonstrate improved adhesion strategies, multifunctional sensing, mechanical durability, and address long-term health monitoring.[66–69]

Signal fidelity and device longevity at the skin–electrode interface are primarily influenced by material properties and mechanical integration. For example, better wearability, reflected by comfort rating scales (CRS) scores ≤4, correlates with dB-level improvements in signal-to-noise ratio for surface electromyography (sEMG) signal acquisition.[70] Skin impedance arising from both resistive and capacitive components must remain stable to enable reliable signal transduction, particularly in biosignal monitoring applications like electromyography (EMG) and electrocardiogram (ECG).[71,72] However, conventional planar metal electrodes often suffer from poor skin conformity and electrochemical instability, leading to increased contact impedance and sensor degradation over time.[73,74]

To mitigate these issues, several strategies have been developed, such as increasing the effective surface area through nanostructured coatings (e.g., platinum nanowires)[75] or integrating hydrogels[76,77] to enhance ionic conductivity or to decrease electrode thickness enabling more intimate contact with the skin.[78] These improvements in interface quality directly translate to enhanced signal-to-noise ratio (SNR), a critical metric for determining the clarity of electrophysiological signals.[66] Electrode size and density must be optimized to balance signal quality, comfort, and spatial resolution; larger sizes lower impedance, while higher densities improve data

resolution but may cause skin irritation.[79,80] These strategies are increasingly being refined in emerging systems that combine high-density, conformal electronics with enhanced biocompatibility.[81]

Adhesive-based attachment limits wear duration due to both biological and mechanical factors. From a biological standpoint, when epidermal turnover, which is manifested in skin cells renewing and building up at the stratum corneum, is obstructed, it can cause skin irritation and will ultimately saturate the adhesive, leading to delamination.[82–85] Skin-safe adhesives for chronic use such as acrylates, silicones, hydrogels, and polyurethane-based systems each present specific tradeoffs in long-term wearability, biocompatibility, and mechanical behavior.[86,87] Acrylate adhesives, while offering strong initial adhesion and compatibility with industrial-scale manufacturing, often lead to skin irritation and epidermal damage over extended use due to their high peel strength and occlusive nature.[88–90] Silicone adhesives provide superior biocompatibility and low trauma upon removal, making them ideal for sensitive skin; however, they typically exhibit lower adhesion strength and reduced durability in humid or high-friction environments.[91–93] Polyurethane-based adhesives balance elasticity and skin conformity but may accumulate sweat and heat at the interface, potentially leading to maceration.[94–96] Adhesive-free van der Waals-based adhesion leverages weak intermolecular forces to achieve reversible and gentle skin contact without chemical adhesives, thereby minimizing irritation and allowing for repeatable use.[83] Microstructured surfaces, inspired by biological systems like gecko feet or beetle pads, are engineered with fine patterns that increase surface area contact and enable conformal attachment through physical interlocking or capillary forces, however large scale deployment and attachment forces are a challenge.[84,97]

Alternative attachment strategies may circumvent these limitations. Circumferential attachment approaches, such as stretchable textile bands, soft wraps, or form-fitting garments, offer promising solutions.[98] These methods distribute pressure more uniformly across a larger surface area, reduce localized stress and shear on the skin, and avoid the occlusive nature of adhesives.[99] Additionally, textile-based or open mesh systems are inherently more breathable and can adapt to skin motion without detaching, thereby enabling chronic monitoring and wearability, especially in ambulatory or active scenarios.[100]

2.4. Power supply

Power supply, as outlined in data analysis and communication section is currently considered the main bottleneck for wearable devices to operate on chronic time scales.[101,102] Conventional battery systems inherently impose bulk and weight that that limit system level design and biointerfaces, as discussed in sections 2.1–2.4.[103] Inherently with capacity of the battery, which scales with bulk, there is a need for recharging depending on power consumption scaling with sampling rate and communication capabilities, which interrupts continuous operation, making batteries alone impractical for high fidelity long-term use.[104] As shown in Fig. 1: power supply section, in a typical high fidelity operation such as multi-channel electrophysiological recording or accelerometry for gait analysis,[105,106] the battery charge decreases steadily throughout the day, requiring recharging approximately every 4–24 hours to maintain functionality.[90] An approach to reduce the burden of conventional battery technology is soft, wearable Li-ion batteries, with an energy density of 538 W h L^{-1},[107] that offer performance levels comparable to their commercial, non-wearable rigid counterparts, as highlighted in comparative studies of power supply in wearables[108–112] but still face challenges in balancing mechanical flexibility with energy storage capacity.[113–115]

An alternate approach is the harvesting of energy using converters of energies to electricity. For example, flexible photovoltaic cells (PVCs) can achieve energy conversion efficiencies of up to 32%[116] under bright indoor lighting and averaging up to 10–15% in full sunlight.[117] Under ASTM G173-03 of 100 mW cm^{-2} and laboratory testing conditions, these cells can generate up to 10–15 mW cm^{-2} of power in direct sunlight exposure, however, in practice this is significantly less, $\sim$0.25 mW cm^{-2}, due to limited time spent in full sunlight. Indoors, bright 1000 Lux warm white light provides 0.318 mW cm^{-2} irradiance,[116] generating 0.1 mW cm^{-2} on-device[116] in lab conditions or 0.027 mW cm^{-2} in practice.[118] Wearable form-factor integration and conversion efficiency loss as cell size increases limits flexible PVC sizes to be reasonably as large as 2–3 cm^2, allowing for energy harvesting up to 1.62 mWh per day indoors or 15 mWh per day outdoors, assuming an average 6 hour charging window. While they provide a reliable power source for outdoor daytime use, their effectiveness depends on season, location, and diminishes significantly indoors or at night, necessitating sufficient energy accumulation during active daylight hours to sustain overnight operation.

Biofuel cells (BFCs) operate with biofluids such as sweat, for energy generation. Sweat lactate-based BFCs exhibit the highest power density, reaching several mW cm^{-2} under lab testing conditions, due to the elevated lactate concentrations in sweat (2–50 mM), however actual system efficiencies are an order of magnitude lower due to changes in sweat rate and lactate dilution, ambient humidity and temperature, and material degradation, with energy densities between 0.2 to 125 μW cm^{-2}.[8,119,120] Work integrating BFCs into wearable form factors shows stable power harvesting at 1–25 mM lactate of 9.7–25 μW[119,121] for short durations ($<$10 minutes) and 10–20 μW[122] over longer durations (ten hours), harvesting 0.1–0.3 mWh per day. Significant difficulties lie in scaling these technologies, especially for long-term wear, given that their delicate, often hydrogel-based composition degrades with exposure to air and elevated temperatures, as outlined in comprehensive reviews of BFC scalability, integration challenges, and materials engineering.[123–126]

Lastly, motion-dependent energy harvesting using piezoelectric (energy produced by mechanical stress/deformation to materials) and triboelectric (energy produced by contact and separation of materials) generators produces intermittent power throughout the day passively from physical body movement.[127]

In wearable implementations, piezoelectric nano generators (PENGs) typically deliver peak open-circuit voltages of 1–10 V and notable peak power outputs up to 1 mW cm^{-2}, but only transiently during motion.[128–130] Under regular biomechanical inputs, the time-averaged power is reduced to 0.01 mW cm^{-2}, depending on the load, force, and movement frequency. With a wearable footprint of 10–1000 cm^2, the power harvested from PENGs can reach 0.1–10 mWh per day, with power generation fluctuating based on activity intensity and duration.[115,131,132] While these methods reduce dependence on external charging, they are highly dependent on environmental conditions such as light availability or temperature gradients, posing challenges for consistent energy supply,[133] with recent comprehensive reviews highlighting state-of-the-art conversion efficiency ($\sim$10–11% for PENGs and $\sim$10–30% for TENGs), biointegration, and energy availability.[134–139]

In contrast with wearable energy harvesters, near-field and far-field wireless power transfer offer significantly higher power availability and consistency. Near-field power harvesting and near-field communication (NFC) operate through proximity interactions between two or more loop antennas, providing on-demand power in short bursts. NFC requires no on-peripheral power supply, as data exchange draws energy from the electromagnetic field generated by an external reader, typically at 13.56 MHz. The NFC forum specifies a wireless charging standard, NFC wireless charging (NFC WLC), which can provide devices with 200–1000 mW wirelessly up to 2 cm away,[140] however higher levels of power transfer would require infrastructure, such as instrumented furniture or tethered tabletop power casters, as battery-powered readers would consume their full capacity in hours. While traditional NFC communication occurs in tens to hundreds of milliseconds, NFC WLC and near field power harvesting can provide power continuously, and with 80–88% typical efficiency and a practical estimate of two to three 3-minute near field interactions per day, can deliver 16–26 mWh per day. These short charging intervals are due to NFC's reliance on tightly coupled antennas, which requires a portable battery-powered reader, such as a modern cell phone, to be affixed to the body at the target site or the wearable and therefore wearer to be practically stationary. Despite NFC's ability to efficiently transfer power, its short transfer distances ($<$2 cm–2 m,[14,141] with large primary coils and high output power) and reliance upon external readers limits operational independence.

Similar to near field wireless charging, far-field radio frequency (RF) power harvesting functions using an electromagnetic field generated by an external device with a transmitting antenna, however at distances an order of magnitude higher,[142] about 1–10 m *versus* $<$2 cm–2 m with NFC. The increased range offers greater flexibility, providing wireless power when a receiving antenna is simply stationary in front of the transmitter. By integrating far-field antennas into wearables, power from commercially available transmitters can be transferred to the wearable device, such as when the wearer is sleeping or working at a desk. Work integrating far-field power harvesting with wearable devices shows around 18–54 mWh per day,[143]

with an average 6-hour charging window. While RF harvesting systems do not require internal power supplies, integrating small batteries into the wearable system offers continuous and consistent energy buffering throughout the day, providing a more reliable power source compared to intermittent energy harvesting methods, making them suitable for low-power wearable devices.

Despite advances in wearable energy harvesters, which are defined by harnessing power from the body or the environment without explicit energy source designed to power them, their performance remains limited, with low energy conversion efficiency, intermittent power supply, and inadequate energy generation (typically $<$0.4 mW day-averaged power).[122,144] These limitations, along with challenges in cost, scalability, biocompatibility, and durability, hinder their practical viability for continuous, long-term use in wearable devices highlighting practical trade-offs in durability, output power, and form factor.[126,135,137,145–153] The integration of hybrid power strategies, combining wireless power transfer with energy harvesting, represents a potential pathway to overcoming these challenges and enabling reliable, long-term operation of wearable sensors.

2.5. Durability

The durability of wearable devices for continuous monitoring is influenced by the inherent material properties and the specific challenges associated with each class of materials used in their design.[154] Fig. 1: durability section outlines key material classes used for wearable device fabrication. Elastomers or textiles are capable of continuous operation over long durations, however they pose an impermeable membrane that prohibits epidermal water loss and epidermal turnover.[155] Silicones, particularly polydimethylsiloxane (PDMS), are inherently prone to mechanical failure at sites of localized stress concentration, such as those introduced by micro-defects, incisions, or inclusions. This vulnerability arises from their low tear strength and limited ability to redistribute strain, making defect propagation a critical mode of failure under cyclic or tensile loading conditions. Alternative elastomers such as polyurethane, styrenic block copolymers, and fluorinated elastomers offer improved tear resistance and mechanical resilience for wearable applications. Textiles, while offering comfort and breathability, encounter durability issues such as fraying and structural breakdown due to repeated wear and washing, which ultimately compromises their functional longevity.[156] In contrast, wearables based on hydrogels, valued for their flexibility and biocompatibility are particularly prone to dehydration, which causes a loss of their intended properties, leading to diminished performance and eventual failure.[157] Therefore careful engineering is required to match material properties with intended use, detailed review articles discuss challenges in substantial detail.[158–162]

2.6. Biosensors

The operational longevity of wearable biosensors varies significantly across sensor types, each with its own set of performance constraints as shown in Fig. 1: biosensors label. Fundamentally, not all biosensors are suitable for chronic use. Electrochemical

sensors, commonly used for detecting metabolites and ionic concentrations, typically exhibit a limited operational window of 3 to 5 days due to issues like biofouling, which compromises their sensitivity and accuracy over time by the accumulation of proteins or other biological material on the electrode surface.[163–165] Gas sensors, employed for detecting volatile compounds such as carbon dioxide (CO_2) or volatile organic compounds (VOCs) may offer an alternative to liquid biomarker to enable continuous monitoring.[166,167] Electrophysiological sensors, which can be categorized into wet and dry interfaces, present further complexities. Wet interface sensors relying on conductive gels or liquids typically operate for only 7 days before suffering from dehydration and adhesion loss that disrupts their electrical contact and reduces measurement fidelity.[168] Dry interface electrical sensors, although capable of operating continuously, are typically limited by inherently higher impedance and susceptibility to motion artifacts, leading to significant signal noise and reduced accuracy during dynamic activities.[58,169,170] Optical sensors are generally considered robust and utilized for monitoring parameters such as blood oxygen levels, however they can be susceptible to signal attenuation caused by light absorption and scattering in biological tissues, which may change over time and should be accounted for in analysis algorithms.[171,172] Biomechanical sensors, which track physical movements and posture, are also considered robust and are used extensively in brick and strap wearable devices. They have been implemented with great success in epidermal electronics leveraging reduced motion artefacts.[173,174] It should be noted that while biophysical methods of detection such as motion and light are considered stable and suitable for chronic operation, their insight is not comprehensive, and enabling the use of electrochemical, electrophysiological, and gaseous detection to operate on chronic timescales may unlock advanced data collection capabilities.

3. Current state of the art approaches to extend operation

Extending the operational lifetime of wearable systems beyond traditional constraints requires coordinated advances across interface design, power delivery, signal acquisition, and data management. This section outlines current state-of-the-art strategies that address these challenges through innovations in biointegration, mechanical stability, wireless power transfer, and chronic biosignal fidelity.

3.1. Biointerfaces

Seamless integration between wearable sensors and the human body relies on specialized attachment mechanisms that ensure stable signal acquisition while preserving natural epidermal turnover and perspiration critical for user comfort. These interfaces are designed to maintain consistent contact, adapt to dynamic skin surfaces, and support long-term monitoring without compromising data accuracy.

3.1.1. Bands. While consumer devices like fitness watches provide activity tracking and heart rate monitoring, their primary focus remains on personal wellness rather than clinical-grade assessments. Because of the mechanical mass of consumer grade device bodies, motion artefacts and impulse response for biophysical measurements limit sensing fidelity. These limitations highlight the need for specialized wearable systems designed to deliver high-fidelity, clinically relevant data. Bands without the rigid device body can provide a mechanically secure attachment for wearable sensors, ensuring stable contact with the skin for accurate data collection mitigating motion artifact challenges outlined in Section 2.3.

An example application of such a soft band, when engineered correctly, is the acquisition of biofluids-such as sweat, tears, or interstitial fluid to obtain biochemical measurements, enabling continuous, non-invasive monitoring of physiological markers.[177–179] This epifluidic platform leverages microfluidic sweat handling to enable monitoring of biochemical markers through on-device colorimetric biofluid analysis. These devices use microfluidic and electrochemical sensing technologies to capture, transport, and analyze sweat, interstitial fluid, or other biofluids directly on the skin.[180,181]

For epidermal microfluidics, adhesives are essential for their function, however they impose a limit for device lifetimes due to epidermal turnover.[100,182] An example of a microfluidic wearable band with an integrated colorimetric timer and biochemical assays for adhesive-free sweat monitoring is demonstrated in Cho et al.[175] Fig. 2(a) shows the microfluidic band and colorimetric sensor suite, which measures pH and lactate concentration using a silver nanoplasmonic assay for lactate monitoring and dye-conjugated silicon dioxide (SiO_2) nanoparticle–agarose composites for pH analysis. The band can be worn on the wrist, forearm, or ankle by stretching the band around the targeted body part (Fig. 2(b)). Fig. 2(c) shows that sweat pH varies during anaerobic exercise, based on tests with iontophoresis-generated sweat from three participants after 100 squats over 10 min. This highlights the ability of the band to monitor dynamic biochemical markers, making it ideal for continuous health monitoring during physical activities.

3.1.2. Biosymbiotics. A remaining challenge for soft bands is the integration of electronics such as radios and microprocessors alongside multimodal sensors, when combined in one functional element the solution resembles current wearables, with already discussed downsides. However, if these individual elements are distributed over a larger area and interconnected in an open mesh-like structure, epidermal turnover, motion artefacts and biosignal quality can be retained. An example of such architecture is shown by Stuart et al.[142] in a device class called biosymbiotics that uses soft, highly conformal electronics personalized via digital fabrication. Using 3D scans or imaging data, these devices achieve optimal sensor placement. Integrated with far-field wireless energy harvesting, they enable long-term, multimodal biosignal acquisition without user intervention mitigating sensor fidelity challenges outlined in Section 2.3. The biosymbiotic architecture also enables the
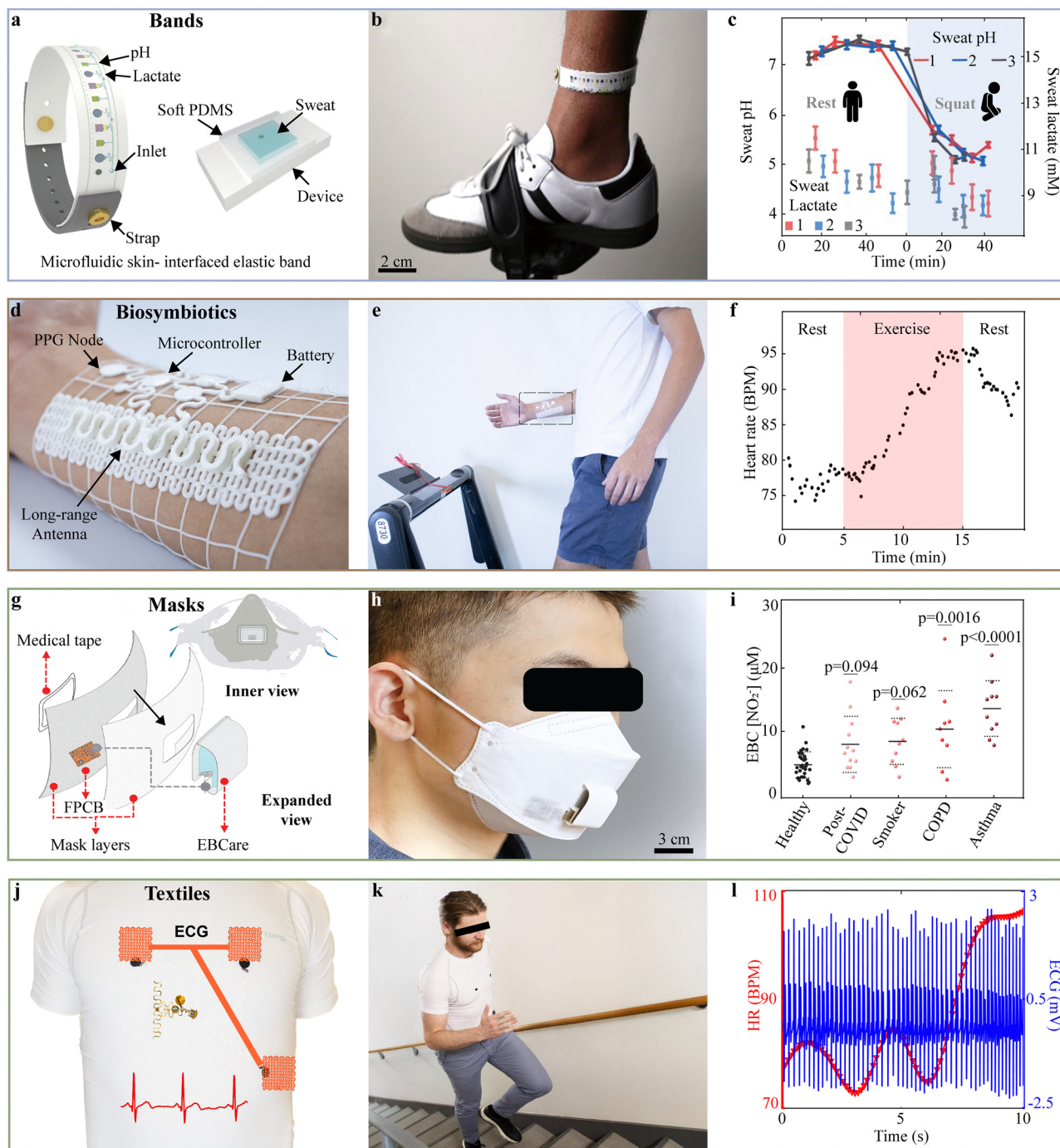
Fig. 2 Current state of the art approaches to extend operation-biointerfaces: (a) schematic of the complete microfluidic skin-interfaced elastic band and rendering of the sweat collection inlet region. (b) Image showing the elastic band device worn on the ankle. (c) Exercise protocol for studying the effect of squatting on sweat pH. (a)–(c) Reproduced from ref. 175 with permission from The American Association for the Advancement of Science, Copyright 2024. (d) Image showing biosymbiotic device attached to the wrist for heart rate and skin temperature recording with functional units labeled. (e) Image of user wearing a long-range biosymbiotic device while walking on a treadmill. (f) Plot of heart rate data extracted from the biosymbiotic device during rest and exercise (red). (d)–(f) Reproduced from ref. 23 with permission from PNAS, Copyright 2023. (g) Schematic showing the expanded and inner views of the smart mask integrated with an EBCare device. (h) Photograph of a fully integrated wireless smart mask worn by a participant. (i) EBC NO_2^- concentration in participants with or potentially with airway inflammation. Statistical analysis of EBC NO_2^- concentration: one-way analysis of variance and Tukey's *post hoc* test. (g)–(i) Reproduced from ref. 176 with permission from the American Association for the Advancement of Science, Copyright 2024. (j) Schematic illustration of electrode positioning and ECG signal acquisition. (k) Subject wearing the textile integrated electrodes while performing daily activity such as climbing the stairs. (l) Plot showing averaged heart rate readings with the same timescale illustrating perturbations to heart rate. (j)–(l) Reproduced from ref. 58 with permission from Wiley-VCH GmbH, Copyright 2024.

integration of RF electronics, usually limited to handheld radios and access points, with tens of miles of communication distance. This is possible because larger areas of the skin can be occupied with antennas that do not disrupt transepidermal water loss, retaining user comfort. Stuart *et al.*[23] realize high-fidelity biosignals transmission of 15 miles without the need for satellite infrastructure. Fig. 2(d) illustrates a biosymbiotic device attached to the wrist for heart rate and skin temperature tracking that is capable of recording data continuously for over weeks without interruption for charging as further discussed in Section 3.5.1. The biosymbiotic long range device is worn by the user during daily activities such as exercising on a treadmill (Fig. 2(e)). The obtained results (Fig. 2(f)) demonstrate the ability to enable high sampling rate measurements during high degrees of motion, showcasing the ability to overcome motion artefacts usually associated with this activity in conventional devices.

3.1.3. Masks. Functionalized face masks have gained significant attention during the Covid-19 pandemic.[183] The mounting location in principle enables the collection of biomarkers difficult or impossible to collect from other areas of the body, such as exhaled gases, offering insights into metabolic activity, hydration status, and disease markers.[184] While this practice is routine in specialized settings such as the integration into a metabolic cart, the bulk of the instrumentation needed is prohibitive for chronic use.[185,186] An example of substantial miniaturization is presented in Heng *et al.*[176] that introduces the concept of exhaled breath condensate (EBC) analysis using a mask-based device (as shown in Fig. 2(g)) for real-time *in situ* monitoring of EBC biomarkers. It integrates a tandem cooling system, automated microfluidics, selective electrochemical biosensors, and a wireless reading circuit, enabling continuous, multimodal tracking of EBC analytes during various indoor and outdoor activities. Continuous condensation of breath required for analysis is enabled by engineered condensation surfaces with evaporative cooling supplied by the breath itself. Fig. 2(h) shows a fully integrated wireless smart mask worn by a participant. Metabolic conditions and respiratory airway inflammation are monitored in healthy individuals, patients with chronic obstructive pulmonary disease or asthma, and those recovering from COVID-19 infection. The data (Fig. 2(i)) demonstrate that elevated EBC NO_2^- levels were observed in groups with airway inflammation, especially asthma patients ($P < 0.0001$), exceeding concentrations in the healthy control group, highlighting its potential for diagnosing, monitoring, and managing respiratory inflammation. Overcoming biofouling challenges discussed in Section 2.6 and epidermal interface frustration described in Section 2.3.

3.1.4. Textiles. Textile-integrated biosensors offer a nonintrusive solution for chronic health monitoring by seamlessly embedding sensing capabilities into everyday clothing.[187,188] The device class potentially enables chronic monitoring; however, it faces limitations from personal hygiene, especially when wear times over multiple weeks are desired. Demonstrations of physiological signal recording, such as heart rate, respiration, hydration, and biochemical markers are recently published.[189]

Advances focus on extending the operational lifespan through power management strategies, self-powered designs, and energy-efficient electronics and addressing durability challenges outlined in Section 2.5.[190,191]

Textile devices that do not require integrated batteries and enable chronic monitoring are RF-enabled technologies that distribute power across the textile from an energy source, usually a smartphone in the pocket of the user, enabling remote and continuous monitoring without requiring adhesive skin contact.[192] These RF systems leverage electromagnetic waves to measure bioimpedance, hydration levels, and even metabolic activity, offering a promising solution for long-term health tracking.[193,194] Chen *et al.* introduce this method by integrating RF power transfer across the textile using embroidered metamaterials with a passive Radio Frequency Identification (RFID) tag, enabling battery-free operation.[195,196] Another example of textile integration is an approach by Clausen *et al.*[58] that monitors electrophysiological biosignals such as ECG by leveraging 3D printing of thermoplastic polyurethane (TPU) directly into the textile, combining biosymbiotic electronic strategies and large body coverage for high-fidelity operation over extended timescales without the limitation of finite battery supply. Fig. 2(j) illustrates TPU based carbon-doped electrodes integrated into textiles that record clinical grade ECG signals. Wear during activity such as climbing the stairs (Fig. 2(k) and (l)) displays heart rate readings (red) alongside ECG signals (blue) during activity, capturing variations in heart rate and demonstrating the stability of the ECG waveform, highlighting the resistance of the system to motion artifacts. Section 4 further discusses that the system is capable of continuous monitoring over days, covering work, activity, and sleep, demonstrating high signal fidelity and accurate heart rate calculations.

3.2. Power supplies

The demanding requirements for thin, soft, skin-interfaced wearable systems described in Section 3 pose challenges and associated research opportunities in power supply and in designs for power-efficient operation. The most prevalent approaches for powering chronic wearables are wireless power transfer[197,198] and ambient power harvesting,[199–202] often specifically tailored towards the application scenario.

3.2.1. Far field RF power. RF power casting offers a scalable solution and is a widely used method for wearable systems, offering recharge at-distance, making it well-suited for on-skin wearable applications.[203–206] Far-field energy harvesting at frequencies of several hundred MHz or GHz enables power transfer over ranges of several meters or more.[207] Far-field approaches typically require directional antennas and are susceptible to reflection and absorption by surrounding materials, including biological tissues. Alignment between the transmission and receiving antennas can be engineered to enable high gain transfer that is efficient, however very directional, or low gain with less alignment sensitivity of sender and receiver.[208] Examples of embodiments utilize small, rigid circuit boards and simple dipole antennas in epidermal form factors to harvest sufficient power for passive sensor data transmission.[203] The most

prevalent frequencies are 915 MHz and 2.4 GHz because they occupy the industrial, scientific, and medical (ISM) radio band that does not require special permits. However, RF power transmission to the human body is subject to regulatory limits to ensure safety. In the United States, the Federal Communications Commission (FCC) restricts the effective isotropic radiated power (EIRP) to 30 dBm[209] at 915 MHz. Moreover, the specific absorption rate (SAR) which quantifies the rate of RF energy absorption by biological tissue is capped at 1.6 W kg^{-1}[210–212] averaged over 1 gram of tissue in the U.S., and 2.0 W kg^{-1} over 10 grams in the EU. These constraints limit the amount of power that can be safely delivered to skin-mounted devices and must be carefully considered in system design. Design strategies must therefore balance angular sensitivity, which is directly linked to antenna gain and therefore power transfer efficiency, transmission duty cycle, and tissue-safe exposure levels.[213] This approach directly addresses the power limitations highlighted in Section 2.4, enabling long-term biosignal acquisition with minimal user burden. Several excellent review articles on the topic cover tradeoffs, designs and applications in detail.[31,43,214,215]

Recent advances that facilitate chronic operation with minimal user interaction are enabled by automated behavioral analysis using neural networks and 3D-printed wearable design for highly personalized, data-driven solutions optimized for specific applications.[216] Stuart et al.[143] introduce a behavioral analysis-driven approach for optimized antenna and rectifier designs, enabling optimized system level designs for high power transfer matched to everyday activities. Key parameters such as orientation, distance, and angular offset relative to power-casting devices are extracted to optimize electromagnetic

performance. Paired with digital manufacturing techniques, this enables the creation of custom rectennas through fused deposition modeling (FDM) printing, ensuring robust, uninterrupted operation of wearable sensors for months without user interaction. Fig. 3(a) shows an example of a rectifier system operating at 915 MHz, enabling single-antenna duplexing for simultaneous wireless power transfer and long-range data communication using a LoRa and maximum power point tracking (MPPT)-enabled power management system. A 7-day experiment averaging 56 mWh per day energy harvesting (Fig. 3(b)) in an urban environment demonstrates long-term operation, with the device continuously running at 5 mHz and recharging near power transmitters placed at the bedside and work desk. Battery voltage data is shown, with green-shaded regions indicating proximity to a power transmitter. Coupled with LoRa communication, high-fidelity biosignals are streamed continuously over 15-mile distances with uninterrupted operation over a week, well beyond limitations imposed by epidermal turn-over discussed in Section 2.3.

3.2.2. Ambient power harvesting. Energy harvesting enables supplementation of battery power in wearable devices but faces practical limitations.[217] Biofuel cells (BFCs) convert chemical energy from sweat[218] and saliva[219] into power through glucose or lactate oxidation, generating 0.2 to 125 μW cm^{-2}, yet require constant skin contact and sufficient biofluid presence, limiting long-term use.[97,119,120,220] Piezoelectric harvesters convert motion into energy, with devices using zinc oxide (ZnO) or lead zirconate titanate (PZT) in soft matrices producing up to 6 V and 0.2 μA cm^{-2} under bending,[221] as outlined in Section 2.4. While these approaches are in principle
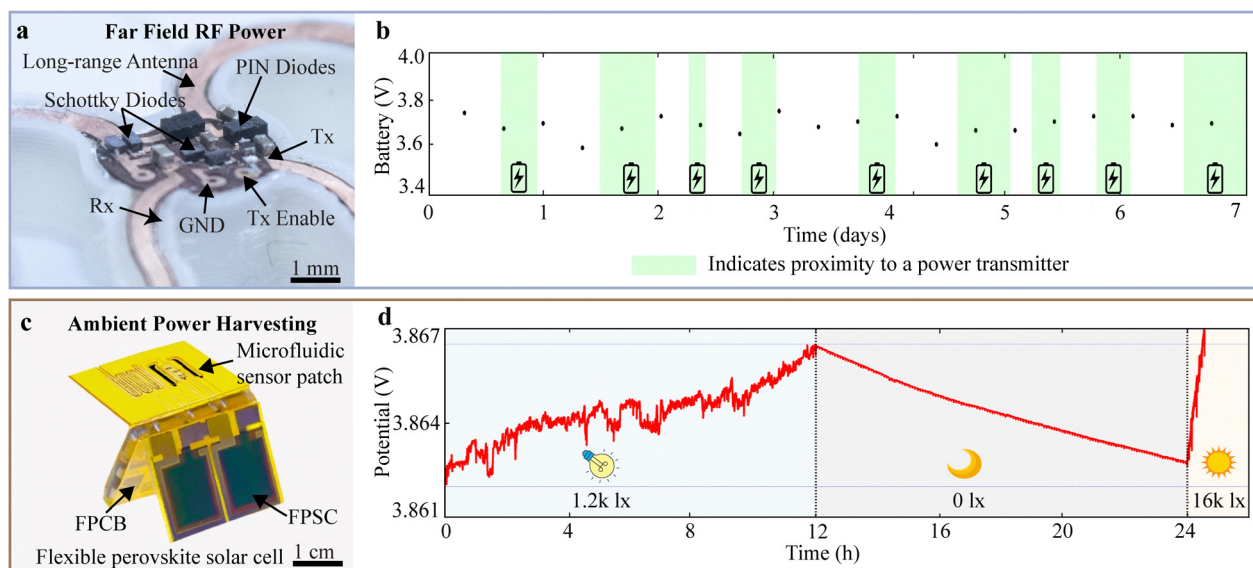
Fig. 3 Current state of the art approaches to extend operation-power supplies: (a) schematic showing single antenna duplexing for simultaneous wireless power transfer and long-range data communication. (b) Plot showing battery voltage monitoring at regular 8-h intervals, with regions shaded in green indicating proximity to a power transmitter for recharging. (a) and (b) Reproduced from ref. 23 with permission from PNAS, Copyright 2023. (c) Image showing the wearable ambient light powered battery-free device assembled in origami style. (d) Data showing operation of battery-aided wearable device for over 24 hours while exposed to various illumination conditions. (c) and (d) Reproduced from ref. 118 with permission from Springer Nature Limited, Copyright 2023.

suitable to create power influx for ultralow-power devices, they have significant challenges in power availability and aim to address the power and recharging challenges described in Section 2.4 by supplementing or replacing batteries.

Fig. 3(c) shows a microfluidic sensing device that is powered by ambient light harvested using perovskite solar cells. The cells are efficient enough to recharge a battery to enable operation even during nighttime with indoor lighting.[118] Over a 24-hour period (Fig. 3(d)), the system harvests on average 2.4 mWh per day while exposed to dynamic lighting environments, including both indoor and outdoor settings, and adjusts its operation based on illumination levels. Experimental trials involved a subject performing diverse physical activities over 12 hours, during which the device intermittently triggered iontophoresis to stimulate sweat and maintain adequate sensor function. To conserve energy, the device dynamically modifies its measurement intervals (ranging from 8 to 60 s) based on available light. This adaptive power management enables uninterrupted data acquisition, processing, and calibration. These results underscore the feasibility of continuous multimodal biosensing over 24 hours, even during sleep, when a small battery is supplemented by solar harvesting to offset low-light periods.

3.3. Biosignals

As discussed in Section 2.6, not all current biosignal acquisition approaches are suitable for chronic operation. This section reviews some of the latest technologies that push the envelope to expand operation beyond current state of the art.

3.3.1. Electrophysiology. The latest electrophysiological sensors feature ultrathin, conformal electrodes paired with wireless communication and low-power electronics, enabling long-term monitoring.[224–226] Recent advances in materials and design mainly focus on epidermal dry electrodes that offer conformal contact and low impedance, without drying issues of conventional gel-based clinical electrodes.[227–229] These electrodes utilize soft elastomeric composites, such as PDMS with CNT fillers or silicone-based materials with metallic nanowires, to reduce contact resistance and enhance signal quality.[148,230] Recent designs, like conductive nanomesh structures made from thin gold films on electrospun polyvinyl alcohol (PVA) fibers, offer high permeability to gases and biofluids while delivering electrophysiological performance comparable to traditional Ag/AgCl gel electrodes with continuous period of 7 days.[231] Tian et al.[232] utilize thin film based devices with serpentine meshes to enable MRI-compatible epidermal-electrophysiology devices with dramatically larger contact areas, and demonstrate their use in controlling prosthetic devices and in monitoring brain function. Epidermal attachment enables artifact-free data collection across five days without requiring removal or interrupting daily activities, such as showering, exercising, working, or sleeping. This approach directly addresses longevity and reliability challenges highlighted in Section 2.6.

Fig. 4(a) shows an example of electrode and system-level engineering that enables electrophysiological signal acquisition. Specifically, biosymbiotic electrodes for electrical impedance

myography (EIM).[58] The system integrates wirelessly powered wearable electronics with carbon-doped TPU filament-based FDM-printed dry electrodes, ensuring stable impedance and seamless biosymbiotic integration. This enables high-fidelity, continuous operation over indefinite timescales. Devices offer long-term wearability (Fig. 4(b)), overcoming the limitations of gel-based adhesive electrodes, as discussed in Section 2.3. Fig. 4(c) demonstrates chronic, high-resolution high-frequency impedance measurements from a subject's forearm over 11 days during a strength training protocol. Data shows a correlation between peak-to-peak impedance profiles and increasing hand dynamometer pulls, with strength gains evident after six days. The uninterrupted epidermal interfacing and stable signal quality highlights the potential of the system for long-term muscle monitoring without requiring conscious interaction.

3.3.2. Body emitted gas. Body-emitted gases contain VOCs and other biomarkers such as humidity and CO_2 that reflect metabolic processes.[233,234] Monitoring these gases offers a non-invasive method for detecting physiological changes, diagnosing diseases, and tracking overall health status.[235,236] Literature on the topic is mostly driven by investigations using room sized equipment such as gas chromatography,[237,238] however recent advances in gas-sensing technologies may enable the real-time detection of specific compounds, providing valuable insights into conditions such as diabetes, metabolic imbalances, and human performance.[182,183,186,239,240]

Recent work by Clausen et al.[222] introduces (Fig. 4(d)) a diffusion-based gas sensor (DBGS) that captures gaseous emissions from the skin using a 3D-printed cavity. The DBGS can measure gas emission rates through differential measurements that are directly correlated to sweat rates, and VOC and CO_2 emissions. Integrated into a biosymbiotic platform capable of 24/7 operation, no adhesives are needed to seal the sensors against the skin, allowing for weeks-long use without user interaction. Positioned on the dorsal forearm, this system provides high temporal resolution and multimodal physiological insights. Chronic data collection (Fig. 4(e)) through 135 hours shows distinct periods of wake, sleep, and activity, with fluctuations in sweat rate corresponding to daily stressors and physical exercises like weightlifting and running. The high temporal resolution (s) allows for new insights into unseen sweat dynamics that highlight delays in sweat with heavy exercise and uncover VOC, CO_2 and sweat dynamics under physiological and psychological stress. Due to the absence of biofouling typically seen in fluidic sensors, this modality is particularly suitable for chronic measurements.

3.3.3. Thermography. Thermoregulation maintains core body temperature within a narrow range of 36–37 °C through sweating, perfusion changes, and shivering. Abnormal temperature patterns can be a powerful biomarker,[241] however, traditional thermography and infrared imaging represent conventional methods of measurement that are not suitable for chronic operation.[242] Emerging ultrathin, skin-integrated sensors leverage advanced materials to enable continuous, high-sensitivity temperature monitoring based on resistive, semiconducting, or optical property changes.[243–245]
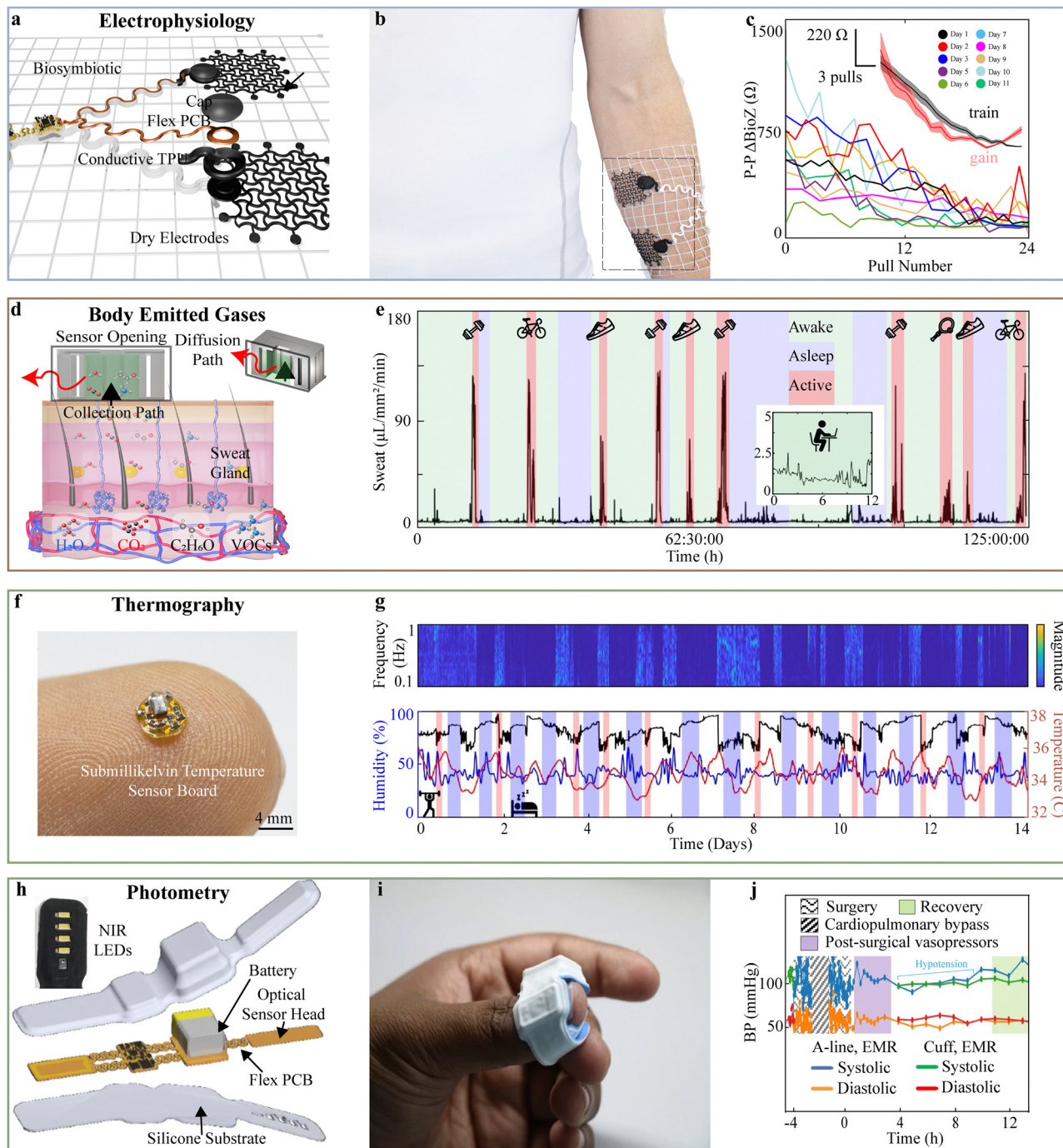
Fig. 4 Current state of the art approaches to extend operation-biosignals: (a) photographic image of a cross-section of a biosymbiotic electrode for electrophysiology. (b) Photographic images of a subject wearing a biosymbiotic electronics integrated device. (c) EIM trends per day following the strength protocol. Inset: Aggregated impedance trendlines for ''train'' data *versus* ''gain'' data for 11 days. (a–c) Reproduced from ref. 58 with permission from Wiley-VCH GmbH, Copyright 2024. (d) Rendered image illustrating gas diffusion through epidermal tissue, originating from the blood vessels and sweat glands. (e) Continuous chronic data collection of sweat rate over one work week using biosymbiotic diffusion-based skin gas analysis with activity marked by icons. Dumbbell: weightlifting session. Bike: cycling activity. Shoe: running activity. Tennis racquet: tennis activity. (d) and (e) Reproduced from ref. 222 with permission from Springer Nature Limited, Copyright 2025. (f) Photographic image of double-sided, sub-millikelvin temperature sensor board, reproduced from ref. 142 with permission from the American Association for the Advancement of Science, Copyright 2021. (g) Data collected from 14-day experiment showing collection of temperature (red) and humidity (blue), and corresponding continuous wavelet transform, reproduced from ref. 143 with permission from Elsevier, Copyright 2023. (h) Exploded rendering of the multispectral device with silicone encapsulation layers, flexible PCB consisting of four islands separated *via* flexible serpentine interconnects, and support circuitry and bottom view of the multiwavelength sensor with multiple pairs of individually controllable broadband and NIR LEDs. (i) Device placement as a finger wrap. (j) A patient monitored for a 12-h period post mitral valve repair was given intravenous epinephrine in response to postoperative hypotension noted in the electronic medical record (EMR). Hour 0 corresponds to the start of surgical wound closure. (h)–(j) Reproduced from ref. 223 with permission from Springer Nature Limited, Copyright 2023.

As discussed in Section 3.1.2., biosymbiotics offer robust skin interfaces without adhesives, offering advantages of epidermal electronics on the chronic timescale Stuart *et al.*,[142] showcase this with sub-millikelvin (< 0.001 K) resolution thermography (Fig. 4(f)), using low thermal mass sensors that enable placement on regions like the axilla. Fig. 4(g) demonstrates the data from a 14-day experiment,[143] where the device continuously monitored temperature and humidity on the bicep. Using continuous wavelet transform, the data reveals distinct patterns of increased contraction frequency during physical exercise (highlighted in red), which corresponds with rises in humidity and local temperature, showcasing perfusion dynamics of the muscle. The device maintains a steady sensing duty cycle of 10 Hz, with minimal data dropout (0.06%), showcasing its ability to provide reliable, long-term monitoring over 14 days.

3.3.4. Photometry. Photoplethysmography (PPG) and pulse oximetry (SpO_2) are the most used sensors in consumer wearables for continuous cardiac monitoring.[246,247] Unlike ECG-based devices (discussed in Section 3.1.4.), PPGs enable signal acquisition from a single contact point.[248]

Multiwavelength PPGs (green, red, infrared) allow data collection from various anatomical sites, with infrared (IR) probing deeper tissues and green light assessing oxygenation.[249] Wristband PPGs are popular for their convenience but face clinical accuracy challenges.[246] To improve performance, recent advances include sensor arrays over radial/ulnar arteries[250] and motion artifact reduction using integrated MEMS sensors.[251]

A frontier in device research is wearable cuffless blood pressure (BP) monitoring using photonic methods; however, this approach remains challenging, with most devices relying on pulse wave velocity (PWV), which correlates arterial stiffness to driving pressure. While promising, PWV is sensitive to factors like physical activity, circadian rhythms, and temperature variations, making it prone to inaccuracies. Franklin *et al.*[223] demonstrate a multinodal, wireless, skin-interfaced system for continuous hemodynamic classification across the BP, cardiac output (CO), and systemic vascular resistance (SVR) coordinate space (as shown in Fig. 4(h)). The system integrates a peripherally worn multiwavelength and multispatial PPG (MWPPG) sensor with a chest-worn device capturing cardiac signals. By combining pulse arrival time (PAT), arteriolar pulse propagation time (reflecting local vascular resistance), and HR, the system can measure and classify physiological changes associated with specific hemodynamic states (Fig. 4(i)). Patients undergoing cardiothoracic surgery often experience post-operative hypotension due to cardiopulmonary bypass and cardiac injury. To prevent cardiogenic shock, vasoconstrictive medications like epinephrine are administered to maintain BP. Fig. 4(j) shows a representative patient's BP trends during epinephrine administration. BP initially stabilizes with the medication but declines as it is tapered off, remaining low for several hours before gradually recovering to pre-surgical levels as the patient recovers from anesthesia, displaying device accuracy.

4. System level demonstrations

As explored in Section 3.3.1., electrophysiological signal acquisition is difficult on chronic timescales.[58] Current roadblocks to a seamless electrophysiology system that can capture critical but short cardiac events are electrode longevity and the high data rate required, which limits battery life. Clausen *et al.* demonstrate a fully integrated, wirelessly powered biosymbiotic platform that enables continuous ECG monitoring with high fidelity during daily activities through power casting electronic technologies described in Section 2.4. (Fig. 5(a)). The result is a system capable of continuous ECG monitoring during daily activities including work, exercise, and sleep. Performance is validated through a 22-hour data recording period with signal-to-noise ratios (SNR) consistently exceeding the 18 dB threshold required for high-quality ECG analysis, averaging around 26.3 dB, as shown in Fig. 5(b). Heart rate data aligns with known physiological events, such as increased rates during activity, a drop during sleep, and a sharp rise upon waking.

In another system level demonstration, Heng *et al.*[176] introduce a mask-based device (EBCare) for real-time monitoring of EBC, shown in Fig. 5(c). The system overcomes the limitation of sweat-based systems by capturing biochemical markers in breath condensate. The system achieves chronic operation through autonomous sample transport with low-power electronics and sensors, supporting long-term, real-time biomarker analysis. Fig. 5(d) shows the long-term usability of EBCare over 14 hours of daily activities, capturing changes in breath biomarkers, where NH_4^+ levels initially dropped after breakfast and spiked after protein-rich lunch and dinner. Alcohol intake caused a rapid rise in EBC alcohol, while NO_2^- levels remained consistently low, indicating reliable, continuous breath analysis.

Capturing high sampling rate data streams chronically is possible with system-level architectures that feature power casting, wireless data transfer, biointerfaces, and sensors that are unaffected by epidermal turnover. Stuart *et al.*[142] showcase a biosymbiotic device capable of continuous multimodal sensing, including temperature and strain data relevant to muscle activity. (Fig. 5(e)). Data in Fig. 5(f) shows that the device returns biosignals during daily activities and sleep, with uninterrupted capture for a 48-hour period. Data reveal elevated thermographic signatures during activity and drops during sleep, reflecting anticipated perfusion changes to the muscle group corroborated by the temporal analysis of the muscle strain signals.

5. Data analysis

As outlined in Sections 2 and 3, for devices operating continuously there is a delicate interplay between data rates, analysis complexity, and communication distance that needs to be carefully managed to enable advanced diagnostic and therapeutic capabilities. Currently this manifests in two fundamental approaches: data analysis on-device and data analysis off-device, each with tradeoffs outlined in Sections 2 and 3.
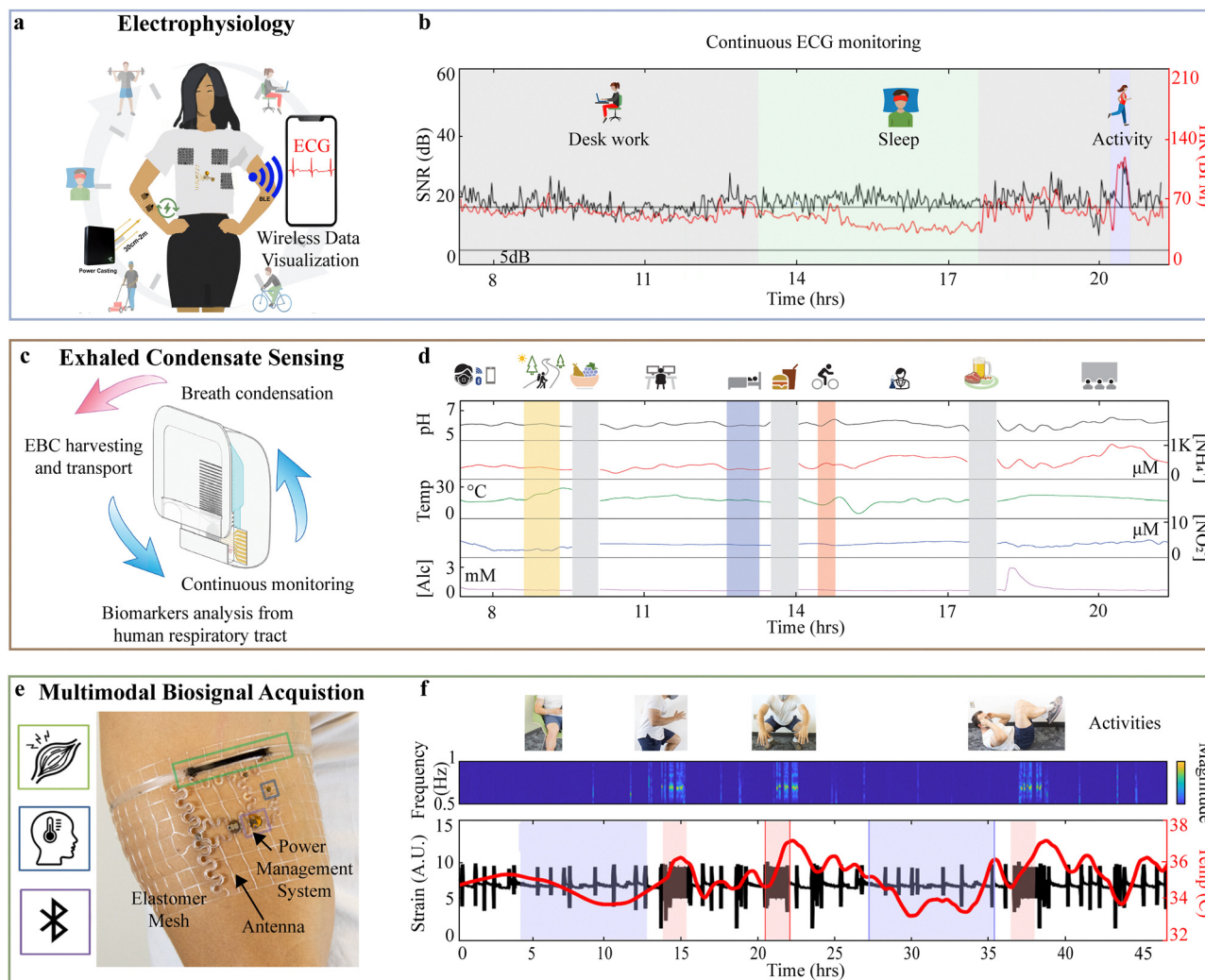
Fig. 5 System level demonstration: (a) illustration of biosymbiotic electrodes integrated with textile and TPU-based electrophysiological biosymbiotic systems, highlighting continuous, around-the-clock data collection. (b) Signal quality and HR plot during continuous monitoring of ECG over a 22-hour data collection period. (a) and (b) Reproduced from ref. 58 with permission from Wiley-VCH GmbH, Copyright 2024. (c) Schematic of a smart EBCare (exhaled breath condensate analysis and respiratory evaluation) mask for efficient harvesting and continuous analysis of exhaled breath condensate. (d) Full-day cross-activity *in situ* EBC analysis of a healthy participant with EBCare monitoring. (c) and (d) Reproduced from ref. 176 with permission from the American Association for the Advancement of Science, Copyright 2024. (e) Illustration of biosymbiotic device with capabilities of multimodal sensing, long-distance, wireless, and battery-free operation. (f) Data collected from 48-hour trial period of continuous recording using biosymbiotic devices. Sleep (shaded blue) and directed calisthenic exercise (shaded red) with continuous wavelet transform of strain signals with discrete changes in frequency corresponding to exercise and visible circadian rhythm and exercise strain – related thermography peaks. (e) and (f) Reproduced from ref. 142 with permission from the American Association for the Advancement of Science, Copyright 2021.
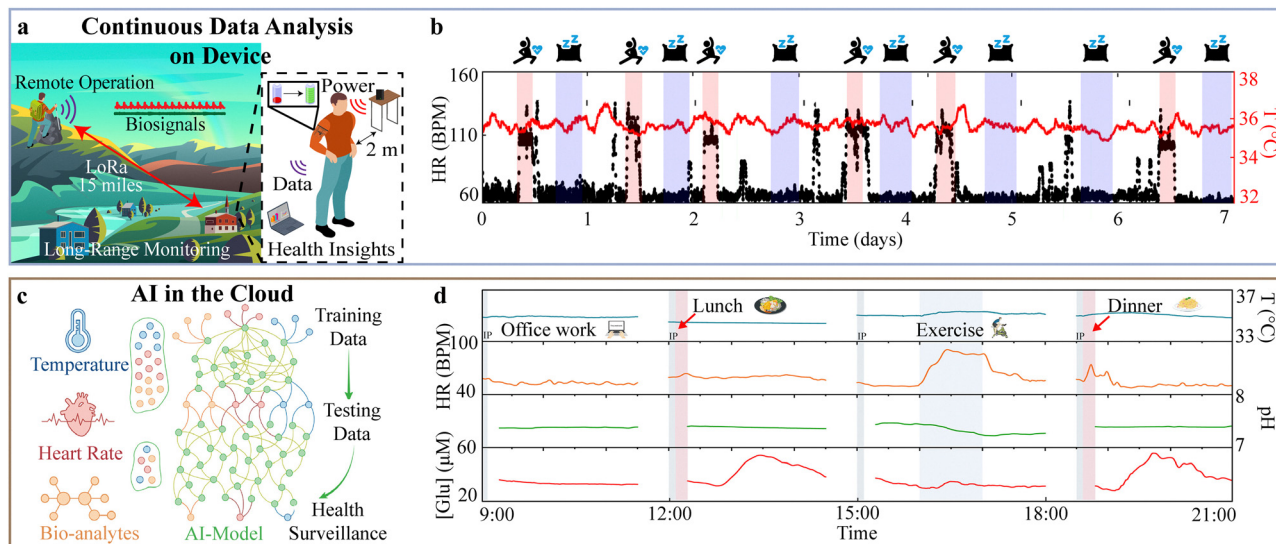
5.1. Continuous data analysis on-device

By leveraging advanced algorithms to extract meaningful trends from large datasets in real time, wearables can deliver valuable insights for both clinical and personal health applications though continuous data analysis on device.[252] When combined with high-fidelity, 24/7 information-rich time series physiological data, this approach enables more accurate diagnostics, early detection of health conditions, and improved patient outcomes.[25,253–255] Stuart *et al.*[26] demonstrates on-device data analysis (Fig. 6(a)), where on-device algorithms capture time series data and extract meaningful biosignal information before wireless transmission. The result is a reduction in sending

events which, in this case using the LoRa communication protocol, amounts to a decrease in the 490.38 mW of power normally consumed during sending events. On-device computation in this case utilizes <3 mW, resulting in net power savings of ~487 mW, enabling continuous operation of the device with wireless recharge at-distance. This continuous, chronic operation over weeks at a time relays critical biomarkers over fifteen miles without satellite or cellular infrastructure. It is important to note that the sampling rate of the sensors is kept high (100 Hz), which is often required for accurate acquisition of fast changing biosignals such as heart rate. The resulting system output does not require cloud computation infrastructure and

Fig. 6 Current state of the art approaches to extend operation-data analysis: (a) schematic of device operation in remote settings with continuous data analysis on device and wireless recharging capabilities. (b) Plot of skin temperature and heart rate recorded during 1 week of continuous data collection and analysis on device. (a) and (b) Reproduced from ref. 23 with permission from PNAS, Copyright 2023. (c) Machine learning-powered multimodal e^3-skin for personalized health surveillance. (d) Full-day physiochemical surveillance of a subject while performing various activities. HR, heart rate; bpm, beats per minute. (c) and (d) Reproduced from ref. 23 with permission from the American Association for the Advancement of Science, Copyright 2023.

can rely on simple data storage frameworks, reducing recurring costs (Fig. 6(b)).

5.2. AI in the cloud and associated challenges

The integration of artificial intelligence (AI) and machine learning (ML), specifically for analysis of time series data in both simple unimodal and complex multimodal models, enables advanced pattern recognition, anomaly detection, and autonomous closed-loop architectures. When coupled with robust datasets representative of the targeted patient population and labels provided by gold standard techniques and/or experts, advanced diagnostic capabilities can be unlocked. This integration is critical for the device class discussed in this review, which produces large amounts of data that are difficult or impossible to review manually. The success of wearables as a next generation diagnostic and therapeutic tool hinges on actionable insights that can lead to meaningful changes in clinical practice.

The use of AI and ML is mostly confined to computation off-device, either on an access point or in the cloud. It's important to note that this typically requires the transmission of raw data, which is energy intensive for biosignals requiring high sampling. Ingested data often requires critical processing steps such as normalization and feature extraction to isolate important patterns in the signal. High numbers of preprocessed samples create a training dataset that, alongside domain expertise, can lead to successful training of models. Once models are generated, new incoming data can be fed to the model to perform inference (identify physiological or disease state) and/or prediction (forecast future physiological or disease states) that can be an asset in treating and managing disease. Recent work integrates this approach with chronic

wearables for early detection of COPD[256] and COVID-19,[257] as well as conditions such as atrial fibrillation,[258] diabetes,[259] and epilepsy.[260]

In a recent example, Song *et al.*[261] introduce a multimodal wearable for machine learning-powered health surveillance (Fig. 6(c)). The 3D-printed epifluidic elastic electronic skin (e^3-skin) integrates electrochemical and biophysical sweat biosensors, iontophoresis electrodes for sweat induction, and microfluidics for sampling electrochemical signals. Powered by a solar cell array and combined with a wireless module, the e^3-skin enables continuous physiochemical data collection from freely moving subjects during daily activities (Fig. 6(d)). AI is central to interpreting the complex, multimodal data collected by the e^3-skin, and its strength is demonstrated during a psychological Go/No-Go test where subjects' reaction time and degree of impairment are assessed while wearing the e^3-skin and drinking 0–2 bottles of beer over 2 hours. Since alcohol tolerance varies between individuals, blood alcohol concentration measurements are not an objective measure of impairment. Multimodal data from the e^3-skin are recorded during the Go/No-Go test, where subjects are asked to classify a shape based on orientation and color. The data are used to train a model which accurately (average 90% and 86%, respectively) predicts an individual's reaction time and degree of impairment (*via* false-positive classification percentage) based solely on biochemical and biophysical data, a feat not possible using gold-standard breathalyzers. Features utilized in training models include heart rate, skin temperature, sweat pH, and sweat alcohol concentration (SAC) extracted using a 30 s moving average window. To account for the physiological delay in sweat secretion, biochemical data are time-shifted by 20 minutes to align with blood concentration of biomarkers. Shapley

additive explanation analysis reveals SAC as the most influential predictor of reaction time, with heart rate required to supplement SAC when predicting degree of impairment, demonstrating how AI supports robust, individualized physiological insights where current approaches cannot provide meaningful conclusions.

6. Clinical utility

Studies show that personalized, data-driven interventions and continuous, objective treatment monitoring often leads to better outcomes than the current standard of care.[263] This section outlines key technological innovations needed for addressing existing challenges and explores specific practical needs of clinicians, aiming to accelerate the seamless integration of wearable devices into clinical workflows for enhanced patient care.

6.1. Integration in clinical workflow

For wearable devices to gain widespread adoption, a basic requirement is data integration into electronic health record (EHR) systems. It is important to note that in the US alone, there are multiple EHR systems (*e.g.*, Epic, Oracle Health, and Meditech), not a single system. Integration is therefore non-trivial, and the level of support for clinical decision-making can vary substantially depending on the EHR platform, because real time alerts are sometimes not included or require additional middleware. Once data is processed and suitably displayed in the EHR, illustrated in Fig. 7(a),[262] visualization and real-time alerts can enhance physician efficiency without increasing their workload. By embedding wearables into routine practice, clinicians can continuously monitor patients and make informed, timely interventions, ultimately improving care delivery.

Integrating wearable digital health technologies (DHTs) into clinical care, if not engineered carefully, presents workflow challenges for both healthcare professionals and patients. Data processing (discussed in Section 5) is critical to offload burden from healthcare workers onto automated, algorithmic analysis.[264,265] The current state of the art deployed in the clinic is retrospective data assessment, which requires substantial effort for incorporation into EHRs because of their lack of standardized, interoperable formats.[266–268]

Wearable manufacturers are increasingly pursuing FDA clearance for class II and class III medical devices, which undergo rigorous clinical testing to meet regulatory standards for safety and efficacy before entering the market, enabling wearables to support clinical decision-making.[269,270] Privacy and security remain major concerns, as most wearable technologies transmit data wirelessly, making it vulnerable to interception.[271] FDA regulations now require robust cybersecurity measures, including encryption, access controls, and regular vulnerability assessments. If devices meet the FDA definition for a "connected device", they require the ability to update firmware after deployment, which limits the use of application-specific integrated circuits (ASICs) without microcontrollers. Depending on device class, manufacturers of FDA-cleared devices must also implement strict privacy protocols, undergo audits, and conduct usability testing with intended users.

Recent additions in the biggest markets in healthcare, such as cardiac and diabetes, include new hardware such as Fourth Frontier's Frontier X Plus, a single-lead, chest-worn ECG monitor using a chest strap, which received FDA 510(k) clearance in November 2024.[272] It provides continuous, real-time cardiac monitoring and uses AI-driven algorithms to detect arrhythmias such as atrial fibrillation and tachycardia.[232] Limitations of such strap-based systems are vulnerable to misalignment during active use with reports stating motion artifacts cause
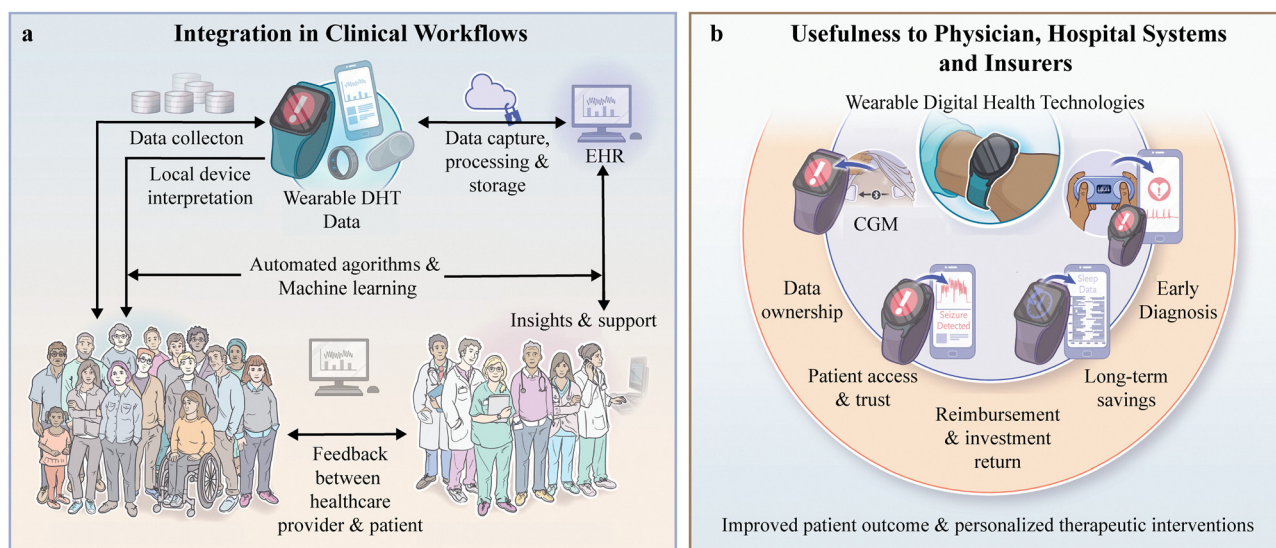
Fig. 7 Current state of the art approaches to extend operation–clinical utility: (a) schematic representation of a wearable digital health technologies integrated into the clinical workflow, and seamless transmission to electronic health records (EHR). (b) Overview of the clinical adoption framework for wearable sensors. Reproduced from ref. 262 with permission from Massachusetts Medical Society, Copyright 2024.

loss in ECG signal for 18.7% of the time leading to false tachycardia detection.[273] While the design of such systems, including the Frontier X Plus, incorporates motion compensation algorithms to mitigate these effects, achieving consistently stable skin contact without adhesives remains an engineering and clinical challenge, which in part, compromises the support of the clinical need to accurately diagnose sporadically occurring cardiac biomarkers of heart failure.[274–278]

In diabetes management, the clinical need is accurate, continuous glucose measurement to guide timely interventions such as insulin dosing, dietary regulation, and lifestyle adjustments. Continuous Glucose Monitors (CGMs) like Dexcom G7 15 Day System, approved in April 2025[279] and Abbott's Libre Rio, cleared in June 2024[280] are the first over-the-counter CGM for adults with Type 2 diabetes and offer minimally invasive, real-time glucose tracking through skin-mounted adhesive patches. However, both systems face persistent real-world challenges. Data shows that ∼19–29%[281] of users experience skin irritation with CGM adhesives, and ∼34–35% report skin lesions,[282] with discomfort leading to device discontinuation in 18–22% of cases,[283] and fill abandonment in ∼3%.[284] Premature detachment from sweat, friction, or movement remains common especially in active users or during water exposure, causing early shutdowns (up to 8.4%), sensor loss (up to 18% in youth), and inaccurate readings. These developments underscore the growing market of clinically validated wearables and their expanding role in managing chronic conditions.[235,236] However, challenges remain in ensuring robust data quality over extended durations, minimizing user burden from recharging or replacement, and expanding sensing capabilities beyond single-parameter tracking. Ultimately, standardized data formats are required to fully leverage data in the EHR, including the ability to tailor visualization to each biosignal to better help physicians understand increasingly meaningful insights from patients. Critical are not only wearables and algorithms that operate 24/7 but also access to data to create more powerful multimodal models that comprehensively analyze patient status to advance diagnostics and therapeutics.[285,286]

6.2. Usefulness to physicians, diagnostics, hospital systems, and insurers

Real-time biosignal monitoring already performed during in-patient hospitalizations can have a significant impact on quality of care when extended into outpatient settings. Alerts for critical events, such as seizures or atrial fibrillation, facilitate timely responses that prevent complications and improve patient outcomes.[287,288] In the long term with the help of comprehensive analysis afforded by modern ML and AI solutions, chronic health insight with clinical grade information may support proactive disease management, reducing the burden of chronic conditions through earlier interventions and more personalized care.

However, while diagnostic value may be evident, without the appropriate incentive structure that facilitates adoption of chronic sensors into the healthcare systems, broad utilization of wearables and mass adoption will rely foremost on demonstrated long-term cost savings (Fig. 7(b)), which may come in

the form of reduced personnel cost or metrics to support value-based care initiatives, a healthcare delivery model that incentivizes providers to improve patient outcomes and reduce costs by linking reimbursement to the quality and efficiency of care rather than the volume of services provided.[262]

Remote monitoring has shown promise in reducing hospital readmissions and streamlining care delivery, resulting in fewer preventable complications and optimized resource utilization,[289,290] however, reimbursement challenges remain.[291] Comparative effectiveness research and clinical trials are essential to validate the benefits of wearable health technologies.[292] Overcoming these hurdles through standardized guidelines and evidence-based policies will be key to driving broader adoption and maximizing the impact of wearables on healthcare efficiency and patient well-being.

7. Conclusions: challenges and prospects

Continuous biosignal acquisition over chronic timeframes requires design strategies that are fundamentally different from those used in short-term monitoring. Systems intended for chronic use must demonstrate stability in signal fidelity, power availability, mechanical integration, and data handling over extended periods, often in uncontrolled environments and across variable user populations.

Recent studies highlight that no single subsystem dictates overall performance longevity. Rather, chronic operation is constrained by the collective interaction of interface, power, biointegration, and data handling. Failure to match requirements in any of these subsystems over time and depending on the anatomical site, physiological state, and activity profile of the user may result in limited usefulness of the wearable.

Devices meeting these requirements can operate stably across multiday to weeks-long periods in clinical and ambulatory environments, maintaining high signal fidelity without the need for user intervention or system recalibration. Recent work shows continuous acquisition of electrophysiological, thermographic, bioimpedance, and gas-emission data during work, rest, and sleep, enabling monitoring under realistic physiological and behavioral conditions. These data capture trends that are inaccessible through short-term measurements, including circadian variation, exercise response, and recovery dynamics.

In clinical workflows, such systems support time-resolved physiological assessments that align with diagnostic and therapeutic windows. Use cases include monitoring of neuromuscular rehabilitation, detection of transient cardiovascular or respiratory abnormalities, and evaluation of therapy efficacy through physiological endpoints. Long-range wireless communication, data reduction on device, and compatibility with standard clinical infrastructure are required to enable seamless integration without disrupting care routines or requiring continuous patient interaction.

These capabilities extend the clinical relevance of wearables from snapshot-based screening tools to platforms that support

longitudinal, personalized health management. To ensure utility at scale, future work may focus on establishing robust validation frameworks, harmonizing data structures for interoperability with electronic health records, and developing clinically actionable analytics that leverage the temporal density of chronic biosignal streams.

Author contributions

A. Bhatia: conceived the figure set and wrote the manuscript. K. A. Kasper: contributed sections to the manuscript, edited, and assisted with calculations. P. Gutruf: conceived, supervised, and wrote the manuscript. All authors have given approval to the final version of the article.

Conflicts of interest

The authors declare no conflict of interest.

Data availability

No primary research results have been included, and no new data was generated or analyzed as part of this review.

Acknowledgements

References

1 Global Growth Insights, Wearable Technology Market Size, Share, Growth, and Industry Analysis, By Types (Augmented Reality, Hearables, Smart Wristband, Smartwatch), By Applications (Enterprise & Industrial, Infotainment, Healthcare & medical, Fitness & wellness), Regional Insights and Forecast to 2033.

2 N. Brasier, J. Wang, W. Gao, J. R. Sempionatto, C. Dincer, H. C. Ates, F. Güder, S. Olenik, I. Schauwecker, D. Schaffarczyk, E. Vayena, N. Ritz, M. Weisser, S. Mtenga, R. Ghaffari, J. A. Rogers and J. Goldhahn, *Nature*, 2024, **636**, 57–68.

3 S. Imani, A. J. Bandodkar, A. M. V. Mohan, R. Kumar, S. Yu, J. Wang and P. P. Mercier, *Nat. Commun.*, 2016, 11650, DOI: **10.1038/ncomms11650**.

4 B. M. A. Yokus and M. A. Daniele, *Biosens. Bioelectron.*, 2021, 113249, DOI: **10.1016/j.bios.2021.113249**.

5 T. Le, F. Ellington, T. Y. Lee, K. Vo, M. Khine, S. K. Krishnan, N. Dutt and H. Cao, *IEEE Access*, 2020, 212478–212498, DOI: **10.1109/ACCESS.2020.3040257**.

6 H. Park, W. Park and C. H. Lee, *NPJ Asia Mater.*, 2021, 23, DOI: **10.1038/s41427-020-00280-x**.

7 J. Kim, A. S. Campbell, B. E. F. de Ávila and J. Wang, *Nat. Biotechnol.*, 2019, 389–406, DOI: **10.1038/s41587-019-0045-y**.

8 M. Amjadi, K. U. Kyung, I. Park and M. Sitti, *Adv. Funct. Mater.*, 2016, 1678–1698, DOI: **10.1002/adfm.201504755**.

9 J. Heikenfeld, A. Jajack, J. Rogers, P. Gutruf, L. Tian, T. Pan, R. Li, M. Khine, J. Kim, J. Wang and J. Kim, *Lab Chip*, 2018, 217–248, DOI: **10.1039/c7lc00914c**.

10 T. R. Ray, J. Choi, A. J. Bandodkar, S. Krishnan, P. Gutruf, L. Tian, R. Ghaffari and J. A. Rogers, *Chem. Rev.*, 2019, 5461–5533, DOI: **10.1021/acs.chemrev.8b00573**.

11 Z. Zhang, L. Wang and C. Lee, *Adv. Sens. Res.*, 2023, 2200072, DOI: **10.1002/adsr.202200072**.

12 T. Wang, Y. Chen, Y. Wang, S. Lee, Y. Lee and J. Dong, *Adv. Sens. Res.*, 2025, 2400142, DOI: **10.1002/adsr.202400142**.

13 M. Smuck, C. A. Odonkor, J. K. Wilt, N. Schmidt and M. A. Swiernik, *NPJ Digit. Med.*, 2021, 45, DOI: **10.1038/s41746-021-00418-3**.

14 T. Stuart, J. Hanna and P. Gutruf, *APL Bioeng*, 2022, **6**, 1–15.

15 V. Vijayan, J. Connolly, J. Condell, N. McKelvey and P. Gardiner, *Sensors*, 2021, 5589, DOI: **10.3390/s21165589**.

16 A. A. Bahashwan, M. Anbar, N. Abdullah, T. Al-Hadhrami and S. M. Hanshi, in Advances in Intelligent Systems and Computing, Springer Science and Business Media Deutschland GmbH, 2021, vol. 1188, pp. 341–353.

17 F. A. Aoudia, M. Magno, M. Gautier, O. Berder and L. Benini, in Proceedings – 19th Euromicro Conference on Digital System Design, DSD 2016, Institute of Electrical and Electronics Engineers Inc., 2016, pp. 200–206.

18 H. Wang and A. O. Fapojuwo, *IEEE Commun. Surv. Tutor.*, 2017, 2621–2639, DOI: **10.1109/COMST.2017.2721379**.

19 R. Katila, T. N. Gia and T. Westerlund, *Comput. Networks*, 2022, 108925, DOI: **10.1016/j.comnet.2022.108925**.

20 D. Ben Arbia, M. M. Alam, Y. Le Moullec and E. Ben Hamida, *Technologies*, 2017, **5**, 1–18.

21 P. Bulić, G. Kojek and A. Biasizzo, *Sensors*, 2019, 3746, DOI: **10.3390/s19173746**.

22 A. Tongkaw, in Implementation of Smart Healthcare Systems using AI, IoT, and Blockchain, Elsevier, 2022, pp. 29–58.

23 T. Stuart, M. Farley, J. Amato, R. Thien, J. Hanna, A. Bhatia, D. M. Clausen and P. Gutruf, *Proc. Natl. Acad. Sci. U. S. A.*, 2023, **120**(50), e2307952120, DOI: **10.1073/pnas.2307952120**.

24 O. Charif and N. Aknin, *ITM Web of Conferences*, 2023, vol. 52, p. 01011.

25 T. Stuart, L. Cai, A. Burton and P. Gutruf, *Biosens. Bioelectron.*, 2021, **178**, 113007.

26 S. Hariprasad and T. Deepa, in Procedia Computer Science, Elsevier B.V., 2020, vol. 171, pp. 2334–2342.

27 F. Adelantado, X. Vilajosana, P. Tuset-Peiro, B. Martinez, J. Melia-Segui and T. Watteyne, *IEEE Communications Magazine*, 2017, **55**, 34–40.

28 L. Casals, B. Mir, R. Vidal and C. Gomez, *Sensors*, 2017, 2364, DOI: **10.3390/s17102364**.

29 J. Li, Y. Zhao, Y. Fan, J. Chen, J. Gong and W. J. Li, *Nano Energy*, 2025, 110821, DOI: **10.1016/j.nanoen.2025.110821**.

30 H. Lewy, *Healthc. Technol. Lett.*, 2015, **2**, 2–5.

31 T. Stuart, J. Hanna and P. Gutruf, *APL Bioeng.*, 2022, 021502, DOI: **10.1063/5.0086935**.

32 V. Vijayan, J. Connolly, J. Condell, N. McKelvey and P. Gardiner, *Sensors*, 2021, 5589, DOI: **10.3390/s21165589**.

33 C. Wall, V. Hetherington and A. Godfrey, *NPJ Digit. Med.*, 2023, 219, DOI: **10.1038/s41746-023-00971-z**.

34 V. Vijayan, J. Connolly, J. Condell, N. McKelvey and P. Gardiner, *Sensors*, 2021, 5589, DOI: **10.3390/s21165589**.

35 O. Durmaz Incel and S. O. Bursa, *IEEE Sens. J.*, 2023, **23**, 5501–5512.

36 F. de Arriba-Pérez, M. Caeiro-Rodríguez and J. M. Santos-Gago, *Sensors*, 2016, 1538, DOI: **10.3390/s16091538**.

37 G. Matsumura, S. Honda, T. Kikuchi, Y. Mizuno, H. Hara, Y. Kondo, H. Nakamura, S. Watanabe, K. Hayakawa, K. Nakajima and K. Takei, *Device*, 2025, 100597, DOI: **10.1016/j.device.2024.100597**.

38 L. Greco, P. Ritrovato and F. Xhafa, *Future Gener. Comput. Syst.*, 2019, **93**, 515–528.

39 L. Menghini, E. Gianfranchi, N. Cellini, E. Patron, M. Tagliabue and M. Sarlo, *Psychophysiology*, 2019, e13441, DOI: **10.1111/psyp.13441**.

40 R. R. Kroll, J. G. Boyd and D. M. Maslove, *J. Med. Internet Res.*, 2016, e253, DOI: **10.2196/jmir.6025**.

41 J. You, M. Lu, L. Dazhen, M. Gao, R. Zhang, W. Li, F. Lei, W. Ren, G. Li and J. Yang, *Adv. Sci.*, 2025, 2414425, DOI: **10.1002/advs.202414425**.

42 L. Gao, Y. Zhang, V. Malyarchuk, L. Jia, K. I. Jang, R. Chad Webb, H. Fu, Y. Shi, G. Zhou, L. Shi, D. Shah, X. Huang, B. Xu, C. Yu, Y. Huang and J. A. Rogers, *Nat. Commun.*, 2014, 4938, DOI: **10.1038/ncomms5938**.

43 J. Heikenfeld, A. Jajack, J. Rogers, P. Gutruf, L. Tian, T. Pan, R. Li, M. Khine, J. Kim, J. Wang and J. Kim, *Lab Chip*, 2018, 217–248, DOI: **10.1039/c7lc00914c**.

44 J. Liang, D. Xian, X. Liu, J. Fu, X. Zhang, B. Tang and J. Lei, *JMIR Mhealth Uhealth*, 2018, e11066, DOI: **10.2196/11066**.

45 Y. Maeda, M. Sekine and T. Tamura, *J. Med. Syst.*, 2011, **35**, 969–976.

46 Y. Gao, H. Li and Y. Luo, *Ind. Manag. Data Syst.*, 2015, 1704–1723, DOI: **10.1108/IMDS-03-2015-0087**.

47 H. Yang, J. Yu, H. Zo and M. Choi, *Telemat. Inform.*, 2016, **33**, 256–269.

48 Y. Li, Y. Sun, Q. Lu, Y. Lu and D. Kong, *Adv. Sens. Res.*, 2024, 2300195, DOI: **10.1002/adsr.202300195**.

49 N. Han, X. Yao, Y. Wang, W. Huang, M. Niu, P. Zhu and Y. Mao, *Biosensors*, 2023, 393, DOI: **10.3390/bios13030393**.

50 R. Wei, H. Li, Z. Chen, Q. Hua, G. Shen and K. Jiang, *npj Flex. Electron.*, 2024, 1–20, DOI: **10.1038/s41528-024-00370-8**.

51 B. E. Song, *Natl. Sci. Rev.*, 2023, nwac191, DOI: **10.1093/nsr/nwac191**.

52 H. L. Cao and S. Q. Cai, *Front. Bioeng. Biotechnol.*, 2022, 1–8, DOI: **10.3389/fbioe.2022.1083579**.

53 Y. Li, Y. Sun, Q. Lu, Y. Lu and D. Kong, *Adv. Sens. Res.*, 2024, 2300195, DOI: **10.1002/adsr.202300195**.

54 N. Han, X. Yao, Y. Wang, W. Huang, M. Niu, P. Zhu and Y. Mao, *Biosensors*, 2023, 393, DOI: **10.3390/bios13030393**.

55 K. M. Halprin, EPIDERMAL TURNOVER TIME-A RE-EXAMINATION, 1972.

56 J. F. Pires-Júnior, T. C. M. Chianca, E. L. Borges, C. Azevedo and G. P. R. Simino, *Rev Lat Am Enfermagem*, 2021, e3500, DOI: **10.1590/1518-8345.5227.3500**.

57 D. Dachev, M. Kazilas, G. Alfano and S. Omairey, *Materials*, 2025, **18**, 2724.

58 D. Clausen, T. Stuart, K. A. Kasper, T. D. McGuire, J. P. Dabdoub, A. Russell, D. Perez, V. Sathishkumaraselvam, A. Miller, S. Roberts and P. Gutruf, *Adv. Funct. Mater.*, 2024, **35**, 2407086, DOI: **10.1002/adfm.202407086**.

59 J. Yin, S. Wang, T. Tat and J. Chen, *Nat. Rev. Bioeng.*, 2024, **2**, 541–558.

60 Y. Zhao, S. Zhang, T. Yu, Y. Zhang, G. Ye, H. Cui, C. He, W. Jiang, Y. Zhai, C. Lu, X. Gu and N. Liu, *Nat. Commun.*, 2021, 1–12, DOI: **10.1038/s41467-021-25152-y**.

61 P. Baker, C. Huang, R. Radi, S. B. Moll, E. Jules and J. L. Arbiser, *Cells*, 2023, 2745, DOI: **10.3390/cells12232745**.

62 S. Liu, J. Zhang, Y. Zhang and R. Zhu, *Nat. Commun.*, 2020, 5618, DOI: **10.1038/s41467-020-19424-2**.

63 Y. Zhang, S. Song, R. Vullings, D. Biswas, N. Simões-Capela, N. Van Hellepute, C. Van Hoof and W. Groenendaal, *Sensor*, 2019, 673, DOI: **10.3390/s19030673**.

64 T. Schweizer and R. Gilgen-Ammann, *JMIR Cardio*, 2025, e67110, DOI: **10.2196/67110**.

65 P. Düking, L. Giessing, M. O. Frenkel, K. Koehler, H. C. Holmberg and B. Sperlich, *JMIR Mhealth Uhealth*, 2020, e16716, DOI: **10.2196/16716**.

66 H. Yeon, H. Lee, Y. Kim, D. Lee, Y. Lee, J.-S. Lee, J. Shin, C. Choi, J.-H. Kang, J. M. Suh, H. Kim, H. S. Kum, J. Lee, D. Kim, K. Ko, S. Ma, P. Lin, S. Han, S. Kim, S.-H. Bae, T.-S. Kim, M.-C. Park, Y.-C. Joo, E. Kim, J. Han and J. Kim, Long-term reliable physical health monitoring by sweat pore-inspired perforated electronic skins, 2021, vol. 7.

67 J. Ma, B. Wen, Y. Zhang, R. Mao, Q. Wu, D. Diao, K. Xu and X. Zhang, *Adv. Funct. Mater.*, 2025, 2425774, DOI: **10.1002/adfm.202425774**.

68 K. Xu, Z. Cai, H. Luo, Y. Lu, C. Ding, G. Yang, L. Wang, C. Kuang, J. Liu and H. Yang, *ACS Nano*, 2024, 26435–26476, DOI: **10.1021/acsnano.4c09062**.

69 H. Zhou, Z. Jin, Y. Xu, Y. Lu, Z. Xia, F. Yang, Q. Wu, Y. Gao, J. Yin, J. Zhang, C. Ni, B. Zhang, Y. He, H. Yang and K. Xu, *Natl. Sci. Rev.*, 2025, nwaf136, DOI: **10.1093/nsr/nwaf136**.

70 F. Amitrano, A. Coccia, G. Pagano, A. Biancardi, G. Tombolini, V. Marsico and G. D'Addio, *Sensors*, 2024, 2763, DOI: **10.3390/s24092763**.

71 D. J. Bora and R. Dasgupta, *IET Syst Biol*, 2020, **14**, 147–159.

72 D. J. Bora and R. Dasgupta, *IET Syst Biol*, 2020, **14**, 292–296.

73 K. Lim, H. Seo, W. G. Chung, H. Song, M. Oh, S. Y. Ryu, Y. Kim and J. U. Park, *Commun. Mater.*, 2024, 49, DOI: **10.1038/s43246-024-00490-8**.

74 K. Goyal, D. A. Borkholder and S. W. Day, *Sensors*, 2022, 8510, DOI: **10.3390/s22218510**.

75 J. Kim, M. Lee, H. J. Shim, R. Ghaffari, H. R. Cho, D. Son, Y. H. Jung, M. Soh, C. Choi, S. Jung, K. Chu, D. Jeon,

S. T. Lee, J. H. Kim, S. H. Choi, T. Hyeon and D. H. Kim, *Nat. Commun.*, 2014, 5747, DOI: 10.1038/ncomms6747.

76 S. J. Oh, T. G. Kim, S. Y. Kim, Y. Jo, S. S. Lee, K. Kim, B. H. Ryu, J. U. Park, Y. Choi and S. Jeong, *Chem. Mater.*, 2016, **28**, 4714–4723.

77 S. W. Shaner, M. Islam, M. B. Kristoffersen, R. Azmi, S. Heissler, M. Ortiz-Catalan, J. G. Korvink and M. Asplund, *Biosens. Bioelectron. X*, 2023, 100143, DOI: 10.1016/j.biosx.2022.100143.

78 L. Yang, L. Gan, Z. Zhang, Z. Zhang, H. Yang, Y. Zhang and J. Wu, *ACS Omega*, 2022, **7**, 13906–13912.

79 K. Lim, H. Seo, W. G. Chung, H. Song, M. Oh, S. Y. Ryu, Y. Kim and J. U. Park, *Commun. Mater.*, 2024, **5**, 49, DOI: 10.1038/s43246-024-00490-8.

80 Z. Turi, G. G. Ambrus, K. A. Ho, T. Sengupta, W. Paulus and A. Antal, *Brain Stimul*, 2014, **7**, 460–467.

81 Q. Li, Y. Li and K. Xu, *Natl. Sci. Open*, 2025, 20240046, DOI: 10.1360/nso/20240046.

82 S. Wang, J. Xu, W. Wang, G. J. N. Wang, R. Rastak, F. Molina-Lopez, J. W. Chung, S. Niu, V. R. Feig, J. Lopez, T. Lei, S. K. Kwon, Y. Kim, A. M. Foudeh, A. Ehrlich, A. Gasperini, Y. Yun, B. Murmann, J. B. H. Tok and Z. Bao, *Nature*, 2018, **555**, 83–88.

83 D.-H. Kim, N. Lu, R. Ma, Y.-S. Kim, R.-H. Kim, S. Wang, J. Wu, S. M. Won, H. Tao, A. Islam, K. J. Yu, T.-I. Kim, R. Chowdhury, M. Ying, L. Xu, M. Li, H.-J. Chung, H. Keum, M. Mccormick, P. Liu, Y.-W. Zhang, F. G. Omenetto, Y. Huang, T. Coleman and J. A. Rogers, *Epidermal Electronics*, 2011, 838–843.

84 J. W. Jeong, W. H. Yeo, A. Akhtar, J. J. S. Norton, Y. J. Kwack, S. Li, S. Y. Jung, Y. Su, W. Lee, J. Xia, H. Cheng, Y. Huang, W. S. Choi, T. Bretl and J. A. Rogers, *Adv. Mater.*, 2013, **25**, 6839–6846.

85 C. Dagdeviren, Y. Shi, P. Joe, R. Ghaffari, G. Balooch, K. Usgaonkar, O. Gur, P. L. Tran, J. R. Crosby, M. Meyer, Y. Su, R. Chad Webb, A. S. Tedesco, M. J. Slepian, Y. Huang and J. A. Rogers, *Nat. Mater.*, 2015, **14**, 728.

86 D. M. Fitzgerald, Y. L. Colson and M. W. Grinstaff, *Prog. Polym. Sci.*, 2023, 101692, DOI: 10.1016/j.progpolymsci.2023.101692.

87 L. Fialho, J. Albuquerque, A. S. Pinho, A. M. Pereira, C. Monteiro, N. Oliveira, S. Ferreira and M. C. L. Martins, *Int. J. Adhes. Adhes.*, 2024, 103636, DOI: 10.1016/j.ijadhadh.2024.103636.

88 J. H. Lee, J. Park, M. H. Myung, M. J. Baek, H. S. Kim and D. W. Lee, *Chem. Eng. J.*, 2021, 126800, DOI: 10.1016/j.cej.2020.126800.

89 I. Márquez, N. Paredes, F. Alarcia and J. I. Velasco, *Polymers*, 2021, 2627, DOI: 10.3390/polym13162627.

90 F. Cilurzo, C. G. M. Gennari and P. Minghetti, *Expert Opin. Drug Delivery*, 2012, 33–45, DOI: 10.1517/17425247.2012.637107.

91 S. C. L. Fischer, K. Kruttwig, V. Bandmann, R. Hensel and E. Arzt, *Macromol. Mater. Eng.*, 2017, 1600526, DOI: 10.1002/mame.201600526.

92 M. Rippon, R. White and P. Davies, Skin adhesives and their role in wound dressings, 2007, pp. 76–86.

93 J. C. del Real, S. L. de Armentia, E. Paz, H. Handwerker and F. Debor, *Advances in Structural Adhesive Bonding*, Elsevier, 2nd edn, 2023, pp. 877–908.

94 W. Liang, N. Ni, Y. Huang and C. Lin, *Polymers*, 2023, 4301, DOI: 10.3390/polym15214301.

95 V. R. Sastri, *Plastics in Medical Devices*, Elsevier, 2022, pp. 381–421.

96 Y. Li, J. Liu, C. Lian, H. Yang, M. Zhang, Y. Wang and H. Dai, *Regen Biomater*, 2024, rbad101, DOI: 10.1093/rb/rbad101.

97 H. Lee, B. P. Lee and P. B. Messersmith, *Nature*, 2007, **448**, 338–341.

98 S. Xu, Y. Zhang, L. Jia, K. E. Mathewson, K.-I. Jang, J. Kim, H. Fu, X. Huang, P. Chava, R. Wang, S. Bhole, L. Wang, Y. J. Na, Y. Guan, M. Flavin, Z. Han, Y. Huang and J. A. Rogers, Soft Microfluidic Assemblies of Sensors, Circuits, and Radios for the Skin, 2014, pp. 70–74.

99 M. J. Yun, Y. H. Sim, D. Y. Lee and S. I. Cha, *Sci. Rep.*, 2021, 4038, DOI: 10.1038/s41598-021-83480-x.

100 S. Choi, H. Lee, R. Ghaffari, T. Hyeon and D. H. Kim, *Adv. Mater.*, 2016, **28**, 4203–4218.

101 S. R. Gambert, *Mayo Clin. Proc. Innov. Qual. Outcomes*, 2006, 112–119, DOI: 10.1016/j.mayocpiqo.2023.08.005.

102 C. Hajat and E. Stein, *Prev. Med. Rep.*, 2018, 284–293, DOI: 10.1016/j.pmedr.2018.10.008.

103 C. M. Lind, J. A. Diaz-Olivares, K. Lindecrantz and J. Eklund, *Sensors*, 2020, **20**, 1–25.

104 M. Jahandar, S. Kim and D. C. Lim, *Nat. Commun.*, 2024, 8149, DOI: 10.1038/s41467-024-52534-9.

105 R. Vatsyayan, J. Lee, A. M. Bourhis, Y. Tchoe, D. R. Cleary, K. J. Tonsfeldt, K. Lee, R. Montgomery-Walsh, A. C. Paulk, U. Hoi Sang, S. S. Cash and S. A. Dayeh, *MRS Bull.*, 2023, 531–546, DOI: 10.1557/s43577-023-00537-0.

106 K. Máthé, A. Tóth, Z. Petykó, I. Szabó and A. Czurkó, *J. Neurosci. Methods*, 2007, **165**, 1–8.

107 L. Yin and J. Wang, *Natl. Sci. Rev.*, 2023, **10**(1), nwac060, DOI: 10.1093/nsr/nwac060.

108 L. Manjakkal, L. Yin, A. Nathan, J. Wang and R. Dahiya, *Adv. Mater.*, 2021, 2100899, DOI: 10.1002/adma.202100899.

109 L. Yin and J. Wang, *Natl. Sci. Rev.*, 2023, nwac060, DOI: 10.1093/nsr/nwac060.

110 J. Li, J. Zhao and J. A. Rogers, *Acc. Chem. Res.*, 2019, **52**, 53–62.

111 M. Gao, P. Wang, L. Jiang, B. Wang, Y. Yao, S. Liu, D. Chu, W. Cheng and Y. Lu, Royal Society of Chemistry, 2021, preprint, DOI: 10.1039/d0ee03911j.

112 Y. Sun, Y. Z. Li and M. Yuan, *Nano Energy*, 2023, 108715, DOI: 10.1016/j.nanoen.2023.108715.

113 Q. Yang, A. Chen, C. Li, G. Zou, H. Li and C. Zhi, *Matter*, 2021, 3146–3160, DOI: 10.1016/j.matt.2021.07.016.

114 J. D. MacKenzie and C. Ho, *Proceedings of the IEEE*, 2015, **103**, 535–553.

115 L. Yin, K. N. Kim, A. Trifonov, T. Podhajny and J. Wang, *Energy Environ. Sci.*, 2022, **15**, 82–101.

116 Y. Cao, Y. Liu, S. M. Zakeeruddin, A. Hagfeldt and M. Grätzel, *Joule*, 2018, **2**, 1108–1117.

117 S. A. Hashemi, S. Ramakrishna and A. G. Aberle, *Energy Environ. Sci.*, 2020, **13**, 685–743.

118 J. Min, S. Demchyshyn, J. R. Sempionatto, Y. Song, B. Hailegnaw, C. Xu, Y. Yang, S. Solomon, C. Putz, L. E. Lehner, J. F. Schwarz, C. Schwarzinger, M. C. Scharber, E. Shirzaei Sani, M. Kaltenbrunner and W. Gao, *Nat Electron*, 2023, **6**, 630–641.

119 A. J. Bandodkar, I. Jeerapan, J. M. You, R. Nuñez-Flores and J. Wang, *Nano Lett.*, 2016, **16**, 721–727.

120 Y. Yu, J. Nassar, C. Xu, J. Min, Y. Yang, A. Dai, R. Doshi, A. Huang, Y. Song, R. Gehlhar, A. D. Ames and W. Gao, Biofuel-powered soft electronic skin with multiplexed and wireless sensing for human-machine interfaces, 2020, vol. 5.

121 L. Yin, K. N. Kim, J. Lv, F. Tehrani, M. Lin, Z. Lin, J. M. Moon, J. Ma, J. Yu, S. Xu and J. Wang, *Nat. Commun.*, 2021, 1542, DOI: **10.1038/s41467-021-21701-7**.

122 L. Yin, J. M. Moon, J. R. Sempionatto, M. Lin, M. Cao, A. Trifonov, F. Zhang, Z. Lou, J. M. Jeong, S. J. Lee, S. Xu and J. Wang, *Joule*, 2021, **5**, 1888–1904.

123 A. J. Bandodkar and J. Wang, *Electroanalysis*, 2016, 1188–1200, DOI: **10.1002/elan.201600019**.

124 T. Stuart, L. Cai, A. Burton and P. Gutruf, *Biosens. Bioelectron.*, 2021, 113007, DOI: **10.1016/j.bios.2021.113007**.

125 N. T. Garland, R. Kaveti and A. J. Bandodkar, *Adv. Mater.*, 2023, **35**, 2303197, DOI: **10.1002/adma.202303197**.

126 A. J. Bandodkar, *J. Electrochem. Soc.*, 2017, **164**, H3007–H3014.

127 M. Pan, C. Yuan, X. Liang, J. Zou, Y. Zhang and C. Bowen, *iScience*, 2020, **23**, 101682, DOI: **10.1016/j.isci.2020.101682**.

128 K. Dong, X. Peng and Z. L. Wang, *Adv. Mater.*, 2020, 1902549, DOI: **10.1002/adma.201902549**.

129 N. Sezer and M. Koç, *Nano Energy*, 2021, 105567, DOI: **10.1016/j.nanoen.2020.105567**.

130 L. Gu, J. Liu, N. Cui, Q. Xu, T. Du, L. Zhang, Z. Wang, C. Long and Y. Qin, *Nat. Commun.*, 2020, 1030, DOI: **10.1038/s41467-020-14846-4**.

131 Jessie Wong, How much electricity can piezoelectric generator produce.

132 2021 IEEE/ACM International Symposium on Low Power Electronics and Design (ISLPED): 26-28 July 2021, IEEE, 2021.

133 R. Yu, S. Feng, Q. Sun, H. Xu, Q. Jiang, J. Guo, B. Dai, D. Cui and K. Wang, *J. Nanobiotechnol.*, 2024, 497, DOI: **10.1186/s12951-024-02774-0**.

134 K. Manojkumar, M. Muthuramalingam, D. Sateesh, S. Hajra, S. Panda, H. J. Kim, A. Sundaramoorthy and V. Vivekananthan, *ACS Appl. Energy Mater.*, 2025, 659–682, DOI: **10.1021/acsaem.4c02268**.

135 Z. L. Wang, *Adv. Energy Mater.*, 2020, 2000137, DOI: **10.1002/aenm.202000137**.

136 B. Yang, Y. Xiong, K. Ma, S. Liu and X. Tao, *EcoMat*, 2020, e12054, DOI: **10.1002/eom2.12054**.

137 L. Manjakkal, L. Yin, A. Nathan, J. Wang and R. Dahiya, *Adv. Mater.*, 2021, 2100899, DOI: **10.1002/adma.202100899**.

138 H. Wu, C. Shan, S. Fu, K. Li, J. Wang, S. Xu, G. Li, Q. Zhao, H. Guo and C. Hu, *Nat. Commun.*, 2024, 6558, DOI: **10.1038/s41467-024-50978-7**.

139 R. A. Whiter, V. Narayan and S. Kar-Narayan, *Adv. Energy Mater.*, 2014, 1400519, DOI: **10.1002/aenm.201400519**.

140 N. Forum, Why Your Next Winning Product Will Use NFC Wireless Charging.

141 P. Lathiya and J. Wang, *Wireless Power Transfer – Recent Development, Applications and New Perspectives*, IntechOpen, 2021.

142 T. Stuart, K. A. Kasper, I. C. Iwerunmor, D. T. McGuire, R. Peralta, J. Hanna, M. Johnson, M. Farley, T. LaMantia, P. Udorvich and P. Gutruf, *Sci. Adv.*, 2021, eabj3269, DOI: **10.1126/sciadv.abj3269**.

143 T. Stuart, X. Yin, S. J. Chen, M. Farley, D. T. McGuire, N. Reddy, R. Thien, S. DiMatteo, C. Fumeaux and P. Gutruf, *Biosens. Bioelectron.*, 2023, 115218, DOI: **10.1016/j.bios.2023.115218**.

144 L. Yin and J. Wang, *Natl. Sci. Rev.*, 2023, nwac060, DOI: **10.1093/nsr/nwac060**.

145 D. Choi, Y. Lee, Z. H. Lin, S. Cho, M. Kim, C. K. Ao, S. Soh, C. Sohn, C. K. Jeong, J. Lee, M. Lee, S. Lee, J. Ryu, P. Parashar, Y. Cho, J. Ahn, I. D. Kim, F. Jiang, P. S. Lee, G. Khandelwal, S. J. Kim, H. S. Kim, H. C. Song, M. Kim, J. Nah, W. Kim, H. G. Menge, Y. T. Park, W. Xu, J. Hao, H. Park, J. H. Lee, D. M. Lee, S. W. Kim, J. Y. Park, H. Zhang, Y. Zi, R. Guo, J. Cheng, Z. Yang, Y. Xie, S. Lee, J. Chung, I. K. Oh, J. S. Kim, T. Cheng, Q. Gao, G. Cheng, G. Gu, M. Shim, J. Jung, C. Yun, C. Zhang, G. Liu, Y. Chen, S. Kim, X. Chen, J. Hu, X. Pu, Z. H. Guo, X. Wang, J. Chen, X. Xiao, X. Xie, M. Jarin, H. Zhang, Y. C. Lai, T. He, H. Kim, I. Park, J. Ahn, N. D. Huynh, Y. Yang, Z. L. Wang, J. M. Baik and D. Choi, *ACS Nano*, 2023, 11087–11219, DOI: **10.1021/acsnano.2c12458**.

146 F. Yi, Z. Zhang, Z. Kang, Q. Liao and Y. Zhang, *Adv. Funct. Mater.*, 2019, 1808849, DOI: **10.1002/adfm.201808849**.

147 C. Wu, A. C. Wang, W. Ding, H. Guo and Z. L. Wang, *Adv. Energy Mater.*, 2019, **9**, 1802906.

148 N. T. Garland, R. Kaveti and A. J. Bandodkar, *Adv. Mater.*, 2023, 2303197, DOI: **10.1002/adma.202303197**.

149 J. Cai, F. Shen, J. Zhao and X. Xiao, *iScience*, 2024, 108998, DOI: **10.1016/j.isci.2024.108998**.

150 V. Leonov, B. Gyselinckx, C. Van Hoof, T. Torfs, R. Firat Yazicioglu, R. J. M. Vullers and P. Fiorini, Wearable self-powered wireless devices with thermoelectric energy scavengers, Conference paper-IEEE Xplore, 2008.

151 S. Olenik, H. S. Lee and F. Güder, *Nat. Rev. Mater.*, 2021, 286–288, DOI: **10.1038/s41578-021-00299-8**.

152 R. Ghaffari, J. Choi, M. S. Raj, S. Chen, S. P. Lee, J. T. Reeder, A. J. Aranyosi, A. Leech, W. Li, S. Schon, J. B. Model and J. A. Rogers, *Adv. Funct. Mater.*, 2020, 1907269, DOI: **10.1002/adfm.201907269**.

153 C. Y. Kim, J. Lee, E. Y. Jeong, Y. Jang, H. Kim, B. Choi, D. Han, Y. Oh and J. W. Jeong, *Adv. Electron. Mater.*, 2025, 2400884, DOI: **10.1002/aelm.202400884**.

154 S. Hong, T. Yu, Z. Wang and C. H. Lee, *Biomaterials*, 2025, 122862, DOI: **10.1016/j.biomaterials.2024.122862**.

155 Q. Liu, P. Lou, Z. Sun, D. Li, H. Ji, Z. Xu, L. Li, J. Xue, R. Wang, Z. Wang and L. Zhang, *Adv. Mater.*, 2025, 2417193, DOI: **10.1002/adma.202417193**.

156 F. Alshabouna, H. S. Lee, G. Barandun, E. Tan, Y. Cotur, T. Asfour, L. Gonzalez-Macia, P. Coatsworth, E. Núnez-Bajo, J. S. Kim and F. Güder, *Mater. Today*, 2022, **59**, 56–67.

157 Y. Liang, A. Offenhäusser, S. Ingebrandt and D. Mayer, *Adv. Healthc. Mater.*, 2021, 2100061, DOI: **10.1002/adhm.2021 00061**.

158 J. Zhu, J. Tao, W. Yan and W. Song, *Natl. Sci. Rev.*, 2023, nwad180, DOI: **10.1093/nsr/nwad180**.

159 T. Shimura, S. Sato, P. Zalar and N. Matsuhisa, *Adv. Electron. Mater.*, 2023, 2200512, DOI: **10.1002/aelm.2022 00512**.

160 S. Park and S. Jayaraman, *Wearable Sensors: Fundamentals, Implementation and Applications*, Elsevier, 2020, pp. 3–27.

161 The engineer's guide to wearables: Lessons learned from design mishaps.

162 M. Brennan, *Device*, 2023, 100096, DOI: **10.1016/j.device. 2023.100096**.

163 M. Madadelahi, F. O. Romero-Soto, R. Kumar, U. B. Tlaxcala and M. J. Madou, *Biosens. Bioelectron.*, 2025, 117099, DOI: **10.1016/j.bios.2024.117099**.

164 H. Duan, S. Peng, S. He, S. Tang, K. Goda, C. H. Wang and M. Li, *Adv. Sci.*, 2023, 2411433, DOI: **10.1002/advs.2024 11433**.

165 I. R. Suhito, K. M. Koo and T. H. Kim, *Biomedicines*, 2021, 1–20, DOI: **10.3390/biomedicines9010015**.

166 A. Hakeem Anwer, M. Saadaoui, A. T. Mohamed, N. Ahmad and A. Benamor, *Chem. Eng. J.*, 2024, 157899, DOI: **10.1016/j.cej.2024.157899**.

167 M. Chen, M. Zhang, Z. Yang, C. Zhou, D. Cui, H. Haick and N. Tang, *Adv. Funct. Mater.*, 2024, 2309732, DOI: **10.1002/adfm.202309732**.

168 X. Wang, Y. Liu, H. Cheng and X. Ouyang, *Adv. Funct. Mater.*, 2022, 2200260, DOI: **10.1002/adfm.202200260**.

169 M. Yamagami, K. M. Peters, I. Milovanovic, I. Kuang, Z. Yang, N. Lu and K. M. Steele, *Sensors*, 2018, 1269, DOI: **10.3390/s18041269**.

170 J. Li, P. Wang and H. J. Huang, *Sensors*, 2020, **20**, 1–18.

171 E. Vavrinsky, N. E. Esfahani, M. Hausner, A. Kuzma, V. Rezo, M. Donoval and H. Kosnacova, *Biosensors*, 2022, 217, DOI: **10.3390/bios12040217**.

172 A. Amjad and X. Xian, *Biosens. Bioelectron.*, 2025, 116844, DOI: **10.1016/j.bios.2024.116844**.

173 X. Wang, H. Yu, S. Kold, O. Rahbek and S. Bai, *Biomim. Intell. Robot.*, 2023, 100089, DOI: **10.1016/j.birob.2023.100089**.

174 P. Morouço, *Int. J. Environ. Res. Public Health*, 2024, **21**, 1126.

175 S. Cho, S. M. Shaban, R. Song, H. Zhang, D. Yang, M.-J. Kim, Y. Xiong, X. Li, K. Madsen, S. Wapnick, S. Zhang, Z. Chen, J. Kim, G. Guinto, M. Li, M. Lee, R. F. Nuxoll, S. Shajari, J. Wang, S. Son, J. Shin, A. J. Aranyosi, D. E. Wright, T. Kim, R. Ghaffari, Y. Huang, D.-H. Kim and J. A. Rogers, A skin-interfaced microfluidic platform supports dynamic sweat biochemical analysis during human exercise, 2024, vol. 16.

176 W. Heng, S. Yin, J. Min, C. Wang, H. Han, E. S. Sani, J. Li, Y. Song, H. B. Rossiter and W. Gao, A smart mask for exhaled breath condensate harvesting and analysis, 2024, pp. 954–961.

177 R. A. Robergs, F. Ghiasvand, D. Parker and D. P. Biochemistry, *Am. J. Physiol.: Regul., Integr. Comp. Physiol.*, 2004, R502–R516, DOI: **10.1152/ajpregu.00114.2004.-The**.

178 G. A. Brooks, *Cell Metab.*, 2018, 757–785, DOI: **10.1016/j.cmet.2018.03.008**.

179 S. Choi, H. Lee, R. Ghaffari, T. Hyeon and D. H. Kim, *Adv. Mater.*, 2016, **28**, 4203–4218.

180 J. Heikenfeld, A. Jajack, B. Feldman, S. W. Granger, S. Gaitonde, G. Begtrup and B. A. Katchman, *Nat. Biotechnol.*, 2019, **37**, 407–419, DOI: **10.1038/s41587-019-0040-3**.

181 B. Paul Kunnel and S. Demuru, *Lab Chip*, 2022, **22**, 1793–1804.

182 L. McNichol, C. Lund, T. Rosen and M. Gray, *J. Wound Ostomy Cont. Nurs.*, 2013, **40**, 365–380.

183 J. Li, J. Yin, S. Ramakrishna and D. Ji, *Biosensors*, 2023, 205, DOI: **10.3390/bios13020205**.

184 Y. Song, X. Wang, L. Wang, L. Qu and X. Zhang, *ACS Sens.*, 2024, 4520–4535, DOI: **10.1021/acssensors.4c01705**.

185 M. Adeel, Y. Cotur, A. Naik, L. Gonzalez-Macia and F. Güder, *Nat. Electron.*, 2022, **5**, 719–720.

186 Z. Yin, Y. Yang, C. Hu, J. Li, B. Qin and X. Yang, *NPJ Asia Mater.*, 2024, 8, DOI: **10.1038/s41427-023-00513-9**.

187 S. Li, H. Li, Y. Lu, M. Zhou, S. Jiang, X. Du and C. Guo, *Biosensors*, 2023, 909, DOI: **10.3390/bios13100909**.

188 F. Michelson, *J. Biomed. Syst. Emerg. Technol.*, 2024, **11**(03), DOI: **10.37421/2952-8526.2024.11.205**.

189 H. A. Rather and M. A. Dar, *Biosensors Nanotheranostics*, 2024, 1–9, DOI: **10.25163/biosensors.317337**.

190 R. Ghaffari, D. S. Yang, J. Kim, A. Mansour, J. A. Wright, J. B. Model, D. E. Wright, J. A. Rogers and T. R. Ray, *ACS Sens.*, 2021, 2787–2801, DOI: **10.1021/acssensors.1c01133**.

191 M. Hemdan, M. A. Ali, A. S. Doghish, S. S. A. Mageed, I. M. Elazab, M. M. Khalil, M. Mabrouk, D. B. Das and A. S. Amin, *Sensors*, 2024, **24**(16), 5143, DOI: **10.3390/s24165143**.

192 C. Luo, I. Gil and R. Fernández-García, *Meas. Sci. Technol.*, 2021, 105112, DOI: **10.1088/1361-6501/ac0ca7**.

193 A. Kandwal, Y. D. Sharma, R. Jasrotia, C. C. Kit, N. Lakshmaiya, M. Sillanpää, L. W. Liu, T. Igbe, A. Kumari, R. Sharma, S. Kumar and C. Sungoum, *Heliyon*, 2024, e37825, DOI: **10.1016/j.heliyon.2024.e37825**.

194 D. K. Vo and K. T. L. Trinh, *Biosensors*, 2024, **14**(11), 560, DOI: **10.3390/bios14110560**.

195 X. Chen, H. He, Z. Khan, L. Sydanheimo, L. Ukkonen and J. Virkki, *IEEE Antennas Wirel. Propag. Lett.*, 2020, **19**, 198–202.

196 X. Chen, H. He, Z. Khan, L. Sydänheimo, L. Ukkonen and J. Virkki, PhotonIcs & Electromagnetics Research Symposium Spring (PIERS SPRING), Rome, Italy, 17–20 June, IEEE Xplore, 2019.

197 H. Sun, Y. Zhang, J. Zhang, X. Sun and H. Peng, *Nat. Rev. Mater.*, 2017, 17023, DOI: **10.1038/natrevmats.2017.23**.

198 J. Kim, A. Banks, H. Cheng, Z. Xie, S. Xu, K. I. Jang, J. W. Lee, Z. Liu, P. Gutruf, X. Huang, P. Wei, F. Liu,

K. Li, M. Dalal, R. Ghaffari, X. Feng, Y. Huang, S. Gupta, U. Paik and J. A. Rogers, *Small*, 2015, **11**, 906–912.

199 A. Tyree, A. Bhatia, M. Hong, J. Hanna, K. A. Kasper, B. Good, D. Perez, D. N. Govalla, A. Hunt, V. Sathishkumaraselvam, J. P. Hoffman, J. W. Rozenblit and P. Gutruf, *Biosens. Bioelectron.*, 2024, 116432, DOI: 10.1016/j.bios.2024.116432.

200 R. A. Bullen, T. C. Arnot, J. B. Lakeman and F. C. Walsh, *Biosens. Bioelectron.*, 2006, 2015–2045, DOI: 10.1016/j.bios.2006.01.030.

201 C. Dagdeviren, F. Javid, P. Joe, T. Von Erlach, T. Bensel, Z. Wei, S. Saxton, C. Cleveland, L. Booth, S. McDonnell, J. Collins, A. Hayward, R. Langer and G. Traverso, *Nat. Biomed. Eng.*, 2017, **1**, 807–817.

202 S. Park, S. W. Heo, W. Lee, D. Inoue, Z. Jiang, K. Yu, H. Jinno, D. Hashizume, M. Sekino, T. Yokota, K. Fukuda, K. Tajima and T. Someya, *Nature*, 2018, **561**, 516–521.

203 Understanding the IoT connectivity landscape: A contemporary M2M radio technology roadmap, 2015.

204 X. Yu, Z. Xie, Y. Yu, J. Lee, A. Vazquez-Guardado, H. Luan, J. Ruban, X. Ning, A. Akhtar, D. Li, B. Ji, Y. Liu, R. Sun, J. Cao, Q. Huo, Y. Zhong, C. M. Lee, S. Y. Kim, P. Gutruf, C. Zhang, Y. Xue, Q. Guo, A. Chempakasseril, P. Tian, W. Lu, J. Y. Jeong, Y. J. Yu, J. Cornman, C. S. Tan, B. H. Kim, K. H. Lee, X. Feng, Y. Huang and J. A. Rogers, *Nature*, 2019, **575**, 473–479.

205 S. Das Barman, A. W. Reza, N. Kumar, M. E. Karim and A. B. Munir, *Renew. Sustain. Energy Rev.*, 2015, 1525–1552, DOI: 10.1016/j.rser.2015.07.031.

206 Development, Biological Effects of fils Radiof requency Radiation.

207 A. P. Sample, D. J. Yeager, P. S. Powledge, A. V. Mamishev and J. R. Smith, *IEEE Trans. Instrum. Meas.*, 2008, **57**, 2608–2615.

208 R. Bansal, The Far-Field: How Far is Far Enough?, *Appl. Microw. Wirel.*, 1999, 58–60.

209 Federal Communications Commission FCC ONLINE TABLE OF FREQUENCY ALLOCATIONS, 2022.

210 SAR Testing, Everything You Should Know About SAR Standards.

211 Federal Communications Commission, Specific Absorption Rate (SAR) for Cellular Telephones.

212 A. Bhatia, J. Hanna, T. Stuart, K. A. Kasper, D. M. Clausen and P. Gutruf, *Chem. Rev.*, 2024, 2205–2280, DOI: 10.1021/acs.chemrev.3c00425.

213 Y. Sun, Y. Z. Li and M. Yuan, *Nano Energy*, 2023, 108715, DOI: 10.1016/j.nanoen.2023.108715.

214 I. Elfergani, A. S. Hussaini, J. Rodriguez and R. Abd-Alhameed, *Antenna fundamentals for legacy mobile applications and beyond*, Springer International Publishing, 2017, DOI: 10.1007/978-3-319-63967-3.

215 B. Yang, Y. Xia, X. Zhi, K. Liu, M. Li and X. Wang, *Device*, 2024, 100246, DOI: 10.1016/j.device.2023.100246.

216 P. Gutruf, *Commun. Mater.*, 2024, 2, DOI: 10.1038/s43246-023-00443-7.

217 How Does Intrinsic Motivation Moderate The Effect of Gamification on The Sustained Use of Wearable Fitness Technology?.

218 W. Gao, S. Emaminejad, H. Y. Y. Nyein, S. Challa, K. Chen, A. Peck, H. M. Fahad, H. Ota, H. Shiraki, D. Kiriya, D. H. Lien, G. A. Brooks, R. W. Davis and A. Javey, *Nature*, 2016, **529**, 509–514.

219 J. E. Mink, R. M. Qaisi, B. E. Logan and M. M. Hussain, *NPG Asia Mater.*, 2014, e89, DOI: 10.1038/am.2014.1.

220 C. Gonzalez-Solino and M. Di Lorenzo, *Biosensors*, 2018, **8**, 11, DOI: 10.3390/bios8010011.

221 J. Chun, N. R. Kang, J. Y. Kim, M. S. Noh, C. Y. Kang, D. Choi, S. W. Kim, Z. Lin Wang and J. Min Baik, *Nano Energy*, 2015, **11**, 1–10.

222 D. Clausen, M. Farley, A. Little, K. Kasper, J. Moreno, L. Limesand and P. Gutruf, *Nat. Commun.*, 2025, 4343, DOI: 10.1038/s41467-025-59629-x.

223 D. Franklin, A. Tzavelis, J. Y. Lee, H. U. Chung, J. Trueb, H. Arafa, S. S. Kwak, I. Huang, Y. Liu, M. Rathod, J. Wu, H. Liu, C. Wu, J. A. Pandit, F. S. Ahmad, P. M. McCarthy and J. A. Rogers, *Nat. Biomed. Eng.*, 2023, **7**, 1229–1241.

224 D.-H. Kim, N. Lu, R. Ma, Y.-S. Kim, R.-H. Kim, S. Wang, J. Wu, S. M. Won, H. Tao, A. Islam, K. J. Yu, T.-I. Kim, R. Chowdhury, M. Ying, L. Xu, M. Li, H.-J. Chung, H. Keum, M. Mccormick, P. Liu, Y.-W. Zhang, F. G. Omenetto, Y. Huang, T. Coleman and J. A. Rogers, *Epidermal Electronics*, 2011, 838–843.

225 S. Ha, C. Kim, Y. M. Chi, A. Akinin, C. Maier, A. Ueno and G. Cauwenberghs, *IEEE Trans. Biomed. Eng.*, 2014, **61**, 1522–1537.

226 S. Xu, Y. Zhang, L. Jia, K. E. Mathewson, K.-I. Jang, J. Kim, H. Fu, X. Huang, P. Chava, R. Wang, S. Bhole, L. Wang, Y. J. Na, Y. Guan, M. Flavin, Z. Han, Y. Huang and J. A. Rogers, Soft Microfluidic Assemblies of Sensors, Circuits, and Radios for the Skin, *Science*, 2014, 70–74.

227 Y. Wang, Y. Qiu, S. K. Ameri, H. Jang, Z. Dai, Y. A. Huang and N. Lu, *npj Flexible Electron.*, 2018, 6, DOI: 10.1038/s41528-017-0019-4.

228 M. A. Lopez-Gordo, D. Sanchez Morillo and F. Pelayo Valle, *Sensors*, 2014, 12847–12870, DOI: 10.3390/s140712847.

229 K. E. Mathewson, T. J. L. Harrison and S. A. D. Kizuk, *Psychophysiology*, 2017, **54**, 74–82.

230 S. M. Lee, H. J. Byeon, J. H. Lee, D. H. Baek, K. H. Lee, J. S. Hong and S. H. Lee, *Sci. Rep.*, 2014, 6074, DOI: 10.1038/srep06074.

231 A. Miyamoto, S. Lee, N. F. Cooray, S. Lee, M. Mori, N. Matsuhisa, H. Jin, L. Yoda, T. Yokota, A. Itoh, M. Sekino, H. Kawasaki, T. Ebihara, M. Amagai and T. Someya, *Nat. Nanotechnol.*, 2017, **12**, 907–913.

232 L. Tian, B. Zimmerman, A. Akhtar, K. J. Yu, M. Moore, J. Wu, R. J. Larsen, J. W. Lee, J. Li, Y. Liu, B. Metzger, S. Qu, X. Guo, K. E. Mathewson, J. A. Fan, J. Cornman, M. Fatina, Z. Xie, Y. Ma, J. Zhang, Y. Zhang, F. Dolcos, M. Fabiani, G. Gratton, T. Bretl, L. J. Hargrove, P. V. Braun, Y. Huang and J. A. Rogers, *Nat. Biomed. Eng.*, 2019, **3**, 194–205.

233 P. C. Moura, M. Raposo and V. Vassilenko, *Biomed. J.*, 2023, 100623, DOI: 10.1016/j.bj.2023.100623.

234 W. Ibrahim, L. Carr, R. Cordell, M. J. Wilde, D. Salman, P. S. Monks, P. Thomas, C. E. Brightling, S. Siddiqui and

N. J. Greening, *Thorax*, 2021, 514–521, DOI: 10.1136/thoraxjnl-2020-215667.

235 Y. Yu, B. Jain, G. Anand, M. Heidarian, A. Lowe and A. Kalra, *Biosens. Bioelectron.*, 2024, 100420, DOI: 10.1016/j.biosx.2023.100420.

236 S. Das and M. Pal, *J. Electrochem. Soc.*, 2020, **167**, 037562.

237 Y. Sekine, S. Toyooka and S. F. Watts, *J. Chromatogr. B: Anal. Technol. Biomed. Life Sci.*, 2007, **859**, 201–207.

238 K. Naitoh, T. Tsuda, K. Nose, T. Kondo, A. Takasu and T. Hirabayashi, *Instrum. Sci. Technol.*, 2002, **30**, 267–280.

239 Md Harun-Or-Rashid, S. Mirzaei and N. Nasiri, *ACS Sens.*, 2025, 1620–1640, DOI: 10.1021/acssensors.4c02843.

240 B. Zong, S. Wu, Y. Yang, Q. Li, T. Tao and S. Mao, *Nanomicro Lett.*, 2025, 54, DOI: 10.1007/s40820-024-01543-w.

241 T. R. Ray, J. Choi, A. J. Bandodkar, S. Krishnan, P. Gutruf, L. Tian, R. Ghaffari and J. A. Rogers, *Chem. Rev.*, 2019, 5461–5533, DOI: 10.1021/acs.chemrev.8b00573.

242 D. A. Kennedy, T. Lee and D. Seely, *Integr. Cancer Ther.*, 2009, 9–16, DOI: 10.1177/1534735408326171.

243 M. Sang, K. Kang, Y. Zhang, H. Zhang, K. Kim, M. Cho, J. Shin, J. H. Hong, T. Kim, S. K. Lee, W. H. Yeo, J. W. Lee, T. Lee, B. Xu and K. J. Yu, *Adv. Mater.*, 2022, 2105865, DOI: 10.1002/adma.202105865.

244 C. Xu, Y. Yang and W. Gao, *Mater*, 2020, 1414–1445, DOI: 10.1016/j.matt.2020.03.020.

245 H. Kim, Y. J. Lee, G. Byun, C. Choi and W. H. Yeo, *Adv. Electron. Mater.*, 2023, 2201294, DOI: 10.1002/aelm.202201294.

246 M. Ghamari, *Int. J. Biosens. Bioelectron.*, 2018, 195–202, DOI: 10.15406/ijbsbe.2018.04.00125.

247 T. Tamura, Y. Maeda, M. Sekine and M. Yoshida, *Electronics*, 2014, 282–302, DOI: 10.3390/electronics3020282.

248 R. Sahni, *Clin. Perinatol.*, 2012, 573–583, DOI: 10.1016/j.clp.2012.06.012.

249 A. R. Kavsaoglu, K. Polat and M. Hariharan, *Appl. Soft Comput. J.*, 2015, **37**, 983–991.

250 IEEE Staff, 2011 IEEE International Conference on Consumer Electronics – Berlin, IEEE, 2011.

251 S. S. Thomas, V. Nathan, C. Zong, K. Soundarapandian, X. Shi and R. Jafari, *IEEE J. Biomed. Health Inform.*, 2016, **20**, 1291–1300.

252 F. M. Surur, A. A. Mamo, B. G. Gebresilassie, K. A. Mekonen, A. Golda, R. K. Behera and K. Kumar, *Data Sci. Manag.*, 2025, DOI: 10.1016/j.dsm.2025.02.004.

253 A. Mahajan, K. Heydari and D. Powell, *NPJ Digit. Med.*, 2025, **8**, 176.

254 S. Shajari, K. Kuruvinashetti, A. Komeili and U. Sundararaj, *Sensors*, 2023, 9498, DOI: 10.3390/s23239498.

255 T. Stuart, K. A. Kasper, I. Christian Iwerunmor, D. T. Mcguire, R. Peralta, J. Hanna, M. Johnson, M. Farley, T. Lamantia, P. Udorvich and P. Gutruf, Biosymbiotic, personalized, and digitally manufactured wireless devices for indefinite collection of high-fidelity biosignals, *Sci. Adv.*, 2021, 7, eabj3269.

256 N. Shehada, J. C. Cancilla, J. S. Torrecilla, E. S. Pariente, G. Brönstrup, S. Christiansen, D. W. Johnson, M. Leja,

M. P. A. Davies, O. Liran, N. Peled and H. Haick, *ACS Nano*, 2016, **10**, 7047–7057.

257 B. Shan, Y. Y. Broza, W. Li, Y. Wang, S. Wu, Z. Liu, J. Wang, S. Gui, L. Wang, Z. Zhang, W. Liu, S. Zhou, W. Jin, Q. Zhang, D. Hu, L. Lin, Q. Zhang, W. Li, J. Wang, H. Liu, Y. Pan and H. Haick, *ACS Nano*, 2020, **14**, 12125–12132.

258 Z. Papalamprakopoulou, D. Stavropoulos, S. Moustakidis, D. Avgerinos, M. Efremidis and P. N. Kampaktsis, *Front. Cardiovasc. Med.*, 2024, 1432876, DOI: 10.3389/fcvm.2024.1432876.

259 E. K. Oikonomou and R. Khera, *Cardiovasc. Diabetol.*, 2023, 259, DOI: 10.1186/s12933-023-01985-3.

260 M. Khan, M. Tom, M. Yasser, T. Basmaji and L. Fraiwan, in 2023 9th International Conference on Optimization and Applications, ICOA 2023 - Proceedings, Institute of Electrical and Electronics Engineers Inc., 2023.

261 Y. Song, R. Y. Tay, J. Li, C. Xu, J. Min, S. Sani, G. Kim, W. Heng, I. Kim and W. Gao, 3D-printed epifluidic electronic skin for machine learning-powered multimodal health surveillance, 2023.

262 G. S. Ginsburg, R. W. Picard and S. H. Friend, *N. Engl. J. Med.*, 2024, **390**, 1118–1127.

263 R. L. Engle, D. C. Mohr, S. K. Holmes, M. N. Seibert, M. Afable, J. Leyson and M. Meterko, *Health Care Manage. Rev.*, 2021, **46**, 174–184.

264 C. Marra, T. Chico, A. Alexandrow, W. G. Dixon, N. Briffa, E. Rainaldi, M. A. Little, K. Size, A. Tsanas, J. B. Franklin, R. Kapur, H. Grice, A. Gariban, J. Ellery, C. Sudlow, A. P. Abernethy and A. Morris, *Lancet Digit Health*, 2024, e225–e231, DOI: 10.1016/S2589-7500(24)00223-1.

265 S. Canali, V. Schiaffonati and A. Aliverti, *PLOS Digit Health*, 2022, e0000104, DOI: 10.1371/journal.pdig.0000104.

266 Mansha Kapoor, Enhancing Patient Care & Health Outcomes with RPM and Wearables.

267 Expert Panel Forbes Councils Member., 14 Emerging Wearable Health Technologies Transforming Remote Care.

268 Y. Liao, C. Thompson, S. Peterson, J. Mandrola and M. S. Beg, *American Society of Clinical Oncology Educational Book*, 2019, pp. 115–121.

269 E. S. Izmailova, J. A. Wagner and E. D. Perakslis, *Clin. Pharmacol. Ther.*, 2018, **104**, 42–52.

270 S. Canali, V. Schiaffonati and A. Aliverti, *PLOS Digit Health*, 2022, e0000104, DOI: 10.1371/journal.pdig.0000104.

271 R. R. Pansare, *J. Emerg. Technol. Innov. Res.*, 2024, **11**, b83–b93.

272 Cardiology Innovations: Frontier X Plus, Chest-Worn ECG Monitor FDA-Cleared for Remote Cardiac Tracking.

273 D. K. Saggu, M. N. Udigala, S. Sarkar, A. Sathiyamoorthy, S. Dash, P. V. R. Mohan, V. Rajan and C. Narasimahan, *Indian Pacing Electrophysiol. J.*, 2024, 282–290, DOI: 10.1016/j.ipej.2024.08.003.

274 H. Wu, G. Yang, K. Zhu, S. Liu, W. Guo, Z. Jiang and Z. Li, *Adv. Sci.*, 2021, 2001938, DOI: 10.1002/advs.202001938.

275 K. Lim, H. Seo, W. G. Chung, H. Song, M. Oh, S. Y. Ryu, Y. Kim and J. U. Park, *ACS Appl. Mater. Interfaces*, 2024, 49, DOI: 10.1038/s43246-024-00490-8.

276 X. Lin, Z. Ou, X. Wang, C. Wang, Y. Ouyang, I. M. Mwakitawa, F. Li, R. Chen, Y. Yue, J. Tang, W. Fang, S. Chen, B. Guo, J. Ouyang, T. Shumilova, Y. Zhou, L. Wang, C. Zhang and K. Sun, *Interdisc. Mater.*, 2024, **3**, 775–790, DOI: **10.1002/idm2.12198**.

277 G. Schiavone and S. P. Lacour, *Sci. Transl. Med.*, 2024, 775–790, DOI: **10.1126/scitranslmed.aaw5858**.

278 T. R. Ray, J. Choi, A. J. Bandodkar, S. Krishnan, P. Gutruf, L. Tian, R. Ghaffari and J. A. Rogers, *Chem. Rev.*, 2019, eaaw5858, DOI: **10.1021/acs.chemrev.8b00573**.

279 Jordyn Bradley, FDA Approves New DexCom Diabetes Device.

280 Abbott, **https://abbott.mediaroom.com/2024-06-10-Abbott-Receives-U-S-FDA-Clearance-for-Two-New-Over-the-Counter-Continuous-Glucose-Monitoring-Systems?**.

281 N. A. M. Asarani, A. N. Reynolds, S. E. Boucher, M. de Bock and B. J. Wheeler, *J. Diabetes Sci. Technol.*, 2020, 328–337, DOI: **10.1177/1932296819870849**.

282 A. K. Berg, K. Nørgaard, J. P. Thyssen, C. Zachariae, E. Hommel, K. Rytter and J. Svensson, *Diabetes Technol. Ther.*, 2018, **20**, 475–482.

283 L. H. Messer, C. Berget, C. Beatson, S. Polsky and G. P. Forlenza, *Diabetes Technol. Ther.*, 2018, **20**, S254–S264.

284 April Hopcroft, 6 Things to Know About Wearing a Continuous Glucose Monitor.

285 A. Awad, S. J. Trenfield, T. D. Pollard, J. J. Ong, M. Elbadawi, L. E. McCoubrey, A. Goyanes, S. Gaisford and A. W. Basit, *Adv. Drug Delivery Rev.*, 2021, 113958, DOI: **10.1016/j.addr.2021.113958**.

286 C. Dinh-Le, R. Chuang, S. Chokshi and D. Mann, *JMIR Mhealth Uhealth*, 2019, e12861, DOI: **10.2196/12861**.

287 T. Stuart, J. Hanna and P. Gutruf, *APL Bioeng.*, 2022, 021502, DOI: **10.1063/5.0086935**.

288 Y. Athavale and S. Krishnan, *Biomed. Signal Process. Control*, 2017, e55534, DOI: **10.1016/j.bspc.2017.03.011**.

289 H. W. Po, Y. C. Chu, H. C. Tsai, C. L. Lin, C. Y. Chen and M. M. Huei-Ming, *JMIR Form. Res.*, 2024, e53455, DOI: **10.2196/53455**.

290 V. K. P. Vudathaneni, R. B. Lanke, M. C. Mudaliyar, K. V. Movva, L. Mounika Kalluri and R. Boyapati, *Cureus*, 2024, **16**(3), e55534, DOI: **10.7759/cureus.55534**.

291 M. Barouni, L. Ahmadian, H. S. Anari and E. Mohsenbeigi, *Sultan Qaboos Univ. Med. J.*, 2020, 260–270, DOI: **10.18295/squmj.2020.20.03.004**.

292 A. Dang and K. Kaur, *Perspect Clin. Res.*, 2016, **7**, 9.